JAMES COOK CYCLONE STRUCTURAL TESTING STATION

CYCLONE TESTING STATION

WIND-INDUCED FATIGUE LOADING ON ROOF CLADDING OF LOW-RISE BUILDINGS

TECHNICAL REPORT NO.41

December 1993

CYCLONE TESTING STATION
JAMES COOK UNIVERSITY OF NORTH QUEENSLAND

WIND-INDUCED FATIGUE LOADING ON ROOF CLADDING OF LOW-RISE BUILDINGS

by

Y. L. Xu

TECHNICAL REPORT NO.41

December 1993

Xu, Y. L. (You Lin), 1952-
Wind induced fatigue loading on roof cladding of low rise buildings

ISBN 0 86443 493 6.
ISSN 0158 - 8338.

1. Roofing, Iron and steel. 2. Wind-pressure. 3. Building, Stormproof. I. James Cook University of North Queensland. Cyclone Testing Station. II. Title. (Series : Technical Report (James Cook University of North Queesnland. Cyclone Testing Station) ; no 41).

690.15

CONTENTS

WIND-INDUCED FATIGUE LOADING ON ROOF CLADDING OF LOW-RISE BUILDINGS

Synopsis

Characteristics of wind loads associated with static or dynamic design of buildings and structures have been extensively investigated in the last two or three decades. The subject of wind-related fatigue design, however, has not been thoroughly explored to date. Only limited knowledge exists in fatigue characteristics of wind loads, particularly in the case of wind loads on low-rise buildings. This report therefore presents a study of wind-induced fatigue loading on roof cladding of low-rise buildings.

The study uses the roof pressures measured on the Texas Tech University Building in the field. Spectra, probability distributions and extreme value distributions of the roof pressures at critical locations are analysed to determine stochastic properties of the pressures. It is found that all the concerned roof pressures could not be modelled as a narrow-band Gaussian process. The rainflow method is therefore used to count load cycles instead of the upcrossing method.

Load cycle histograms of the pressures exhibit fatigue characteristics of the pressure itself, and they are closely related to stochastic properties of the pressure. Total load cycle distributions are then computed using load cycle histograms in consideration of long-term effects of wind climate. The results show that the total load cycle distribution in temperate regions is significantly different from that in tropical cyclone regions, and the total number of cycles is dependent on the parameters associated with the description of wind climate.

Probability analysis shows that as far as cycle mean levels are concerned, most cycles in the total load cycle distribution are concentrated in a certain area. The statistical average of the cycle mean levels for a given cycle range is suggested as an equivalent mean level for this cycle range so that the resulting fatigue test procedure of roof cladding becomes practical.

Finally, the present results are compared with the load cycle distributions currently used in Australia and Europe. A number of comments has been made with respect to fatigue design criteria, wind regions, distributions of cycle ranges and numbers of cycles.

1 INTRODUCTION

1.1 Wind-Induced Fatigue Damage to Structures

Fatigue is the term used to describe the material or structure failure caused by repeated load which is less than the ultimate static failure load. Wind pressures and forces on structures are strongly fluctuating due to the natural turbulence in incident wind and the turbulence induced by the interaction between the incident wind and the structure. Therefore, sustained strong wind could cause fatigue damage to structures or structure components.

On Christmas day 1974, the tropical cyclone Tracy passed over Darwin, a north Australian City. Tracy was an intense cyclone moving particularly slowly, so that the city was subjected to strong winds for about 4 hours. A large percentage of the houses and buildings were so badly damaged that they had to be demolished and reconstructed. Over 90% of houses and 70% of other structures suffered a significant loss of roof cladding (Walker, 1975). Subsequent field investigations and laboratory tests showed that fatigue failure in the vicinity of roof fasteners was the only possible cause of the severe roofing damage (Beck and Stevens, 1976; Morgan and Beck, 1977; Beck and Stevens, 1979; and Mahendran, 1990)

The Kemper Arena is a large auditorium in Kansas City, Missouri, that houses sporting and civic events. On 4th June 1979, a local thunderstorm caused a large portion of the roof to collapse. A postdisaster investigation carried out by Stratta (Liu, 1991) concluded that fatigue failure of one of the large bolts that connected the roof to the space frame above the roof caused progressive failure of the roof. It is one of the few cases in which fatigue has been identified as the cause of failure of a major building.

The investigation into the wind-induced collapse of the 381 m high guyed steel mast Emley Moor in 1969 also revealed that a tensile failure of one of the leg joints initiated the collapse of the mast. The possibility of fatigue damage in the tension-prone joints, however, was not taken into account until 1987, when the Welding Institute of United Kingdom was commissioned by the Independent Broadcasting Authority (IBA) to undertake full-scale fatigue test of welded joints and on-site measurements of wind speed and stresses in the joints (Lambert, Ogle and Smith, 1988).

As a consequence of such events and others, several wind-induced load cycle distributions were recommended for predicting fatigue life and

performing fatigue tests of structures.

1.2 Existing Load Cycle Distributions

Immediately after cyclone Tracy, the Darwin Area Building Manual (DABM, 1975) incorporated a provision that any roofing systems approved for reconstruction and new construction in Darwin should be proof-tested for fatigue resistance. The prototype test of roof assemblies consisted of 10,000 cycles of repeated load, with the load varying from zero to the permissible design load which corresponded to the wind speed of a 50-year return period multiplied by a 'cyclone multiplier' of 1.15. Following the repeated load test, the roof assembly was to be subject to a static load from zero to 1.8 times the design load (see Table 1.1).

TABLE 1.1 Load Cycle Distributions Used in Australia and UK for Roof Cladding

DABM (Cyclone Regions)		TR440 (Cyclone Regions)		BRE (Temperate Regions)	
Percentage of peak load (1)	Number of cycles (2)	Percentage of peak load (3)	Number of cycles (4)	Percentage of peak load (5)	Number of cycles (6)
Apply once		Apply once		Apply five times	
100%	10,000	62.5% 75% 100%	8,000 2,000 200	90% 40% 60% 59% 80% 70%	1 960 60 240 5 14
Apply once		Apply once		Apply once	
180%	1	Ultimate Load	1	100%	1

Note: Peak load in DABM and TR440 is the permissible design load; Peak load in BRE corresponds to a 50-year return period; Ultimate load in TR440 is 1.6 times the peak load for three or more tests, 1.8 times the peak load for two tests and 2.0 times the peak load for one test.

There was a considerable body of opinion that the DABM load cycle distribution was too severe. Later, Melbourne (1977) used the upcrossing method to analyse wind-induced response of typical structures and structure components, and he suggested two types of load cycle distributions: one for a Gaussian process and the other for an intermittent process. The two load cycle distributions are listed in Table 1.2, in which p_m, p_{rms} and p^* are the mean pressure, root mean square pressure and peak pressure, respectively. Both load cycle distributions suggested by Melbourne were substantially modified at a workshop hosted by the Commonwealth Department of Construction, Australia, and two compromise distributions of load cycles were produced for tropical cyclone regions (TR440, 1977; Beck, 1978). Table 1.1 shows the TR440 load cycle distribution for roof cladding. Since then the TR440 load cycle distribution has been largely adopted in Australian cyclone regions, and written into the Australian Wind Loading Code (SAA, 1989).

In the upcrossing method, all peaks in a time-history record are simply treated as cycles. In an attempt to count actual cycle range and mean levels of roof pressures, Beck and Stevens (1979) used a 'discriminate range-counting method' to count a one-hour critical roof pressure record taken in a wind tunnel on a 1:300 scale model of a low-rise building with a 10° pitch roof, and they proposed another load cycle distribution listed in Table 1.2.

TABLE 1.2 Proposed Load Cycle Distributions (after Cook, 1990)

Source: Use: Rate: Mean: Rms: (1)	Melbourne Gaussian 1000 cycles/hr $p_m=0.5p^*$ $p_{rms}=0.125p^*$ (2)	Melbourne Intermittent 5000 cycles/hr $p_m=0.25p^*$ $p_{rms}=0.094p^*$ (3)	Beck and Steven Intermittent 2770 cycles/hr $p_m=0.15p^*$ $p_{rms}=0.115p^*$ (4)
Composition of cycles in one hour			
	1 @$p_m\pm4p_{rms}$ 10 @$p_m\pm3p_{rms}$ 100 @$p_m\pm2p_{rms}$ 899 @$p_m\pm p_{rms}$	5 @$p_m\pm8p_{rms}$ 50 @$p_m\pm6p_{rms}$ 500 @$p_m\pm4p_{rms}$ 1000 @$p_m\pm2p_{rms}$ 3445 @$p_m\pm p_{rms}$	5 @$p_m+0.75p_{rms}$ to $p_m+7.25p_{rms}$ 25 @$p_m+2.5p_{rms}$ to $p_m+5.5p_{rms}$ 70 @0 to $p_m+5.25p_{rms}$ 400 @$p_m+0.5p_{rms}$ to $p_m+3.5p_{rms}$ 70 @0 to $p_m+3.25p_{rms}$ 1800 @0 to $p_m+1.5p_{rms}$ 400 @0 to $p_m+0.5p_{rms}$

Although the TR440 load cycle distribution has been adopted in most of cyclone-prone areas in Australia, the Northern Territory of Australia has rejected the TR440 recommendation with the argument that some of roof assemblies passing the TR440 test seem little different from those which failed in cyclone Tracy. The DABM load cycle distribution is still used now in the Northern Territory of Australia.

In North America and Europe, the wind-induced load cycle distributions for temperate regions associated with large scale weather systems are significantly different from those used in Australia for cyclone regions. More than 25 years ago, Davenport (1966) proposed an analytical method to estimate wind-induced fatigue damage to structures. This method is based on a narrow-band Gaussian process but it includes the long-term effect of wind climate on structure fatigue. By using this analytical method, a simple relationship between the gust response factor and fatigue damage was later derived by Dionne and Davenport (1988). Also using Davenport's procedure, the European Convention for Construction Steelwork (ECCS) gave recommendations for wind-induced fatigue loading (ECCS, 1987). The ECCS wind-induced load cycle distributions were reproduced by Cook (1990) in terms of the number of cycles exceeding levels of load expressed as percentage of the peak design load and they are shown in Fig. 1.1.

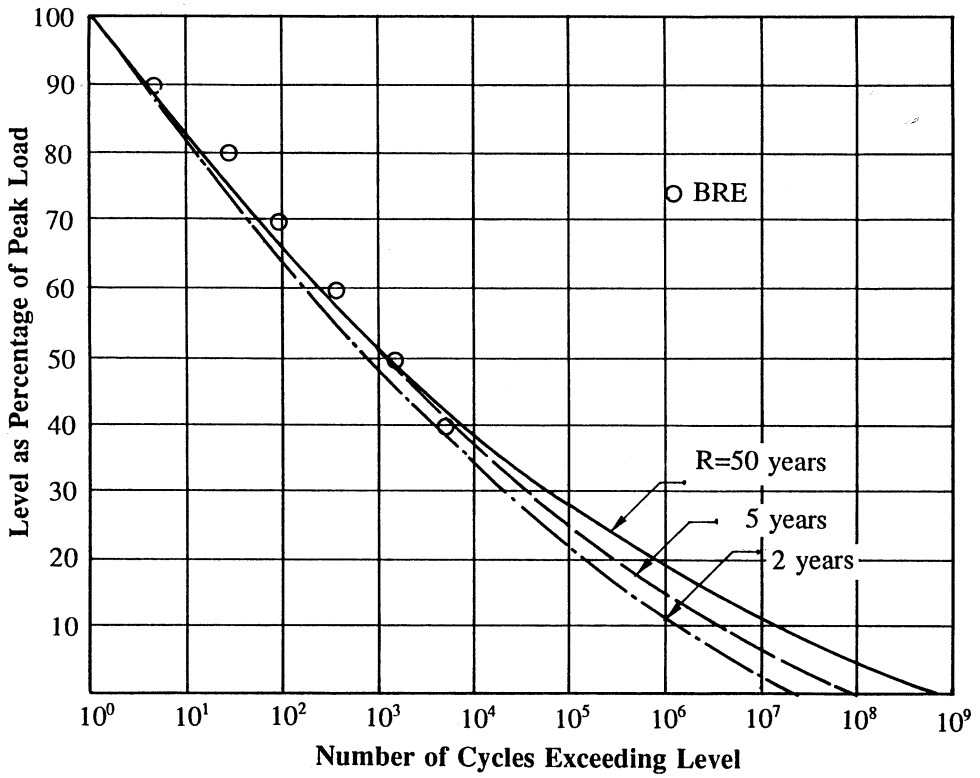

FIG.1.1 ECCS RECOMMENDATIONS FOR WIND-INDUCED FATIGUE LOADING (AFTER COOK, 1990)

Considering that most wind pressures on a building are not a narrow-band Gaussian process, Lynn and Stathopoulos (1985) proposed a hybrid Gaussian-Weibull extreme model to evaluate the number of load cycles and the fatigue damage during one storm. This model is still largely based on the upcrossing method. The UK Building Research Establishment (BRE), on the other hand, derived a load cycle distribution for temperate regions by counting peak loads obtained from both the 20 strongest storms in a 50-year return period in the UK and the Mth highest peak fluctuations in each storm (Cook, 1990). The resulting load cycles were broken into five batches and given in a mixed order in an attempt to represent the natural mixed occurrence (see Table 1.1). The cumulative distribution of this sequence is also superimposed on Fig. 1.1, and it can be seen that the distribution is almost identical to the low-cycle range of the ECCS recommendations.

Fig. 1.2 shows the frequency distributions of both wind speed and wind stagnation pressure, recommended in the draft of the German wind loading code for zone II (FRG recommendation, Gerhardt and Kramer, 1986). The frequency distribution of wind speeds is derived from the extreme value distribution of wind speeds with a 50-year return period. Based on the frequency distribution of wind pressure shown in Fig. 1.2, Gerhardt and Kramer (1986) suggested two methods for simulating fatigue loading: quasi-static approach and peak factor approach. The total load cycles in both methods for a 50-year return period consist of ten batches. The load cycle distribution in each batch is shown in Fig. 1.3.

It is apparent that there is a considerable difference between the aforementioned load cycle distributions. With particular reference to wind-induced fatigue loading on roof cladding, some comments are given in the next section.

1.3 Problems Associated with Roof Cladding

Wind loads applied on the roof of a low building are determined by the interaction between the incident wind and the building itself. With a flat roof, the wind flow normal to a wall separates at the upwind edge and may reattach at some distance downwind to form separation bubbles as cylindrical vortices. At all other wind angles, conical 'delta-wing' vortices may develop from the upwind corner of the building. The roof pressures under these vortices are strongly negative and fluctuating, and they dominate the design of the roof cladding.

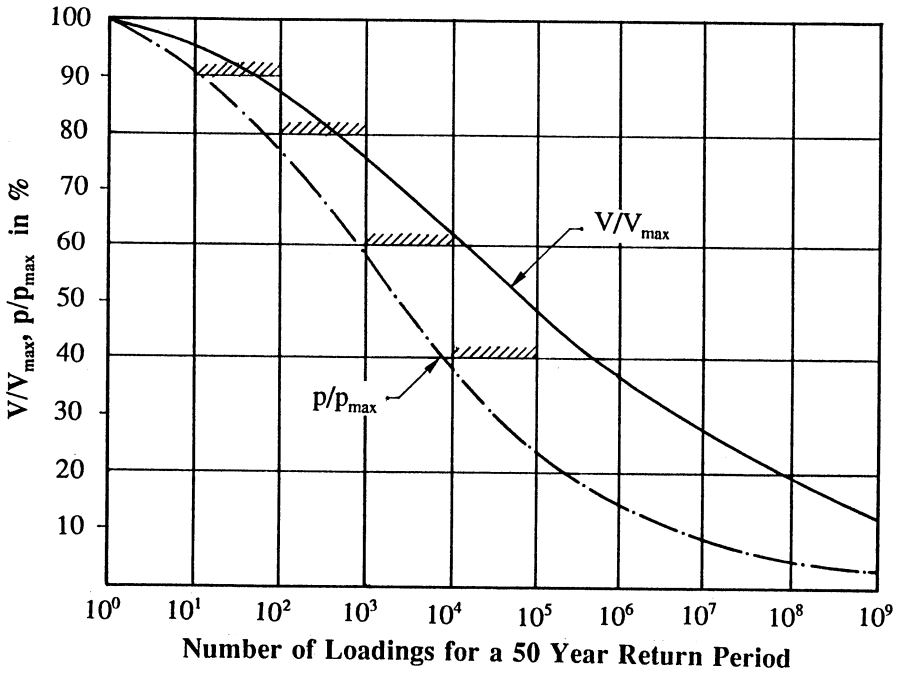

FIG.1.2 FRG FREQUENCY DISTRIBUTIONS OF WIND SPEED AND WIND PRESSURE (AFTER GERHARDT AND KRAMER, 1986)

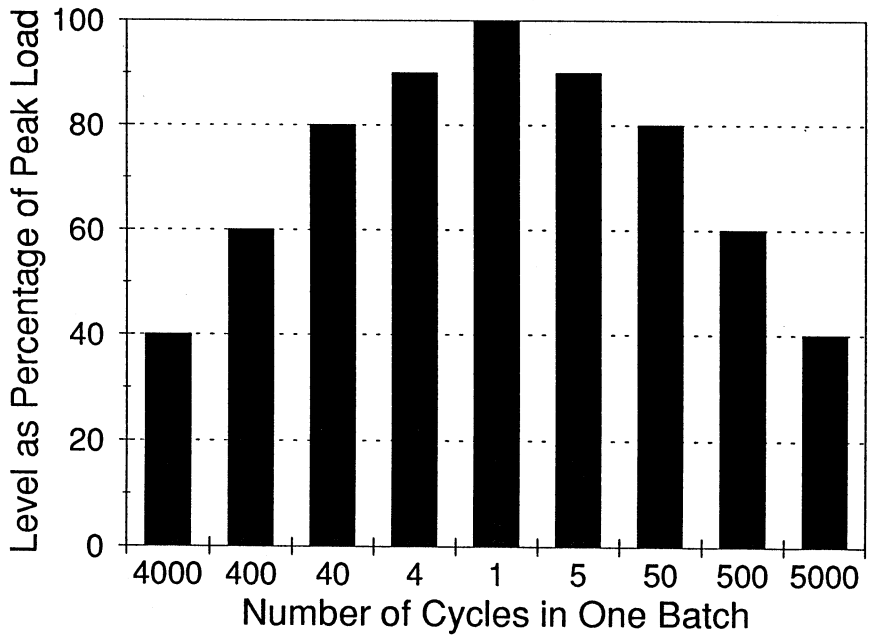

FIG.1.3 LOAD CYCLE DISTRIBUTION IN ONE BATCH (AFTER GERHARDT AND KRAMER, 1986)

One problem as far as fatigue loading is concerned is stochastic properties of these roof pressures. If the pressure is a stationary and narrow-band Gaussian process, the number and distribution of load cycles are nearly the same as those of the peak pressures, and they can be estimated by the upcrossing method (Robson, 1963). If the pressure is a broad-band non-Gaussian process, it is hardly possible to employ the upcrossing method to count load cycles as closed hysteresis loops and to eliminate small pressure amplitude variations. Therefore, stochastic properties of the roof pressures should be identified first in order that a reasonable method can be employed to count load cycles.

Wind-induced fatigue damage to metal structures actually accumulates from storm to storm and from year to year. This is particularly true for the structures in temperate regions (Vickery, 1992). In tropical cyclone regions, wind conditions controlled by large scale weather systems may not provide significant fatigue problem. However, the accumulation of fatigue damage from cyclone to cyclone during the design life of roof cladding should be taken into account. Therefore, probability distributions of wind speed in temperate regions and extreme value distributions of cyclones must be clarified and integrated into the procedure for estimating the number and distribution of load cycles.

It is well known that both magnitude and distribution of wind pressures on a roof depend on many parameters, such as roof slope, architectural features, terrain roughness and surrounding environment (Stathopoulos, 1984). Effects of these parameters lead to different peak pressures for the static or dynamic design of roof cladding. The effects have been also considered in the existing load cycle distributions in terms of peak loads. However, the effects on the number and distribution of load cycles have not been taken into account. It is necessary to carry out the corresponding investigations in order to provide a rational and economical fatigue design of roof cladding.

1.4 Aims and Limitations of the Research Project

The broad aim of the research project described in this report is to investigate wind-induced fatigue loading on roof cladding of low-rise buildings. More special goals are as follows:

(a) to ascertain stochastic properties of roof pressures at critical locations, and to find a cycle count method if the roof pressures are not a narrow-band Gaussian process.

(b) to identify basic characteristics of the number and distribution of load cycles for roof pressures, and to establish a rational procedure for determining total load cycles of the pressure in consideration of long-term effects of wind climate.

(c) to find characteristics of total load cycle distributions as far as the mean levels of cycles are concerned, and to perform a parametric study of total load cycle distributions with respect to pressure tap positions on the roof, wind return periods, wind speed distributions in temperate regions, extreme value distributions of cyclones, and design life of roof cladding.

(d) to compare the present results with the load cycle distributions currently used in Australia and Europe, and to make comments on these distributions with respect to design criteria, wind regions, distributions of cycle ranges and numbers of cycles.

This study uses the roof pressures measured on the Texas Tech University Building (TTU Building) in the field. Available roof pressures of two- or three-hour consecutive records are limited so that effects of wind speed and direction on fatigue characteristics of pressures, and effects of roof slope, terrain roughness and internal pressures on total load cycle distributions could not be investigated. All these limitations are expected to be overcome when the required data are available.

2 STOCHASTIC PROPERTIES OF ROOF PRESSURES

2.1 Roof Pressures Measured on TTU Building

The TTU Building provides the best opportunity yet to study wind effects on full-scale low buildings. Sufficient details on the TTU Building have been given by Levitan and Mehta (1992a and 1992b), and Yeatts and Mehta (1992). Some information relevant to this study is briefly repeated here.

The building is a 9.1 x 13.7 x 4.0 m rotatable metal building. The surrounding terrain is flat and open. More than 8 almost consecutive 15-minute records for each of three critical pressure taps (taps 50123, 50101 and 50501) have been provided by the Wind Engineering Research Field Laboratory of the Texas Tech University. The pressure on the tap 50123 was recorded at the upwind roof edge with wind normal to the wall of the building. The pressures on the taps 50101 and 50501 were recorded on the

upwind roof corner with wind angle of approximate 45° relative to both corner walls. All the three taps were under the "delta-wing" vortices or cylindrical vortices, and they had strongly negative pressures. The building configuration and the tap locations are shown in Fig. 2.1.

The Validyne pressure transducers were used to measure the roof pressures on the taps 50101 and 50501 whilst the OMEGA pressure transducer was used for the tap 50123. All pressure transducers were sampled at 40 Hz. The Validyne and OMEGA transducers were low-pass filtered at 10 Hz and 8 Hz, respectively. The instruments measuring both wind speed and wind direction were sampled at 10 Hz and low-pass filtered at 8 Hz. The computer system converted all data in the pressure coefficient form using the 15-minute mean wind speed at the roof height. The mean, root mean square and peak pressure coefficients as well as the corresponding mean wind speed are listed in the Table 2.1 for the average of 8 records. The pressure coefficients in the time-history are shown in Fig. 2.2. It is obvious that there are significant differences in pressure traces. All pressure records used in this study correspond to a stationary wind speed and wind direction.

2.2 Spectrum Analysis of Roof Pressures

Although roof pressure data collected at the TTU Building have been analysed by Mehta et al (1991, 1992) and have been compared with the results obtained from the wind tunnel model tests of the TTU Building (Surry, 1991; Cochran and Cermark, 1992; and Okada and Ha, 1992), limited information on the pressure spectra is available.

Figs. 2.3 to 2.5 show, respectively, the normalised power spectra of pressure fluctuations at the taps 50123, 50101 and 50501. The corresponding longitudinal turbulence spectra of incident wind are also plotted. It can be seen that the significant pressure fluctuation energy in each tap distributes over a wide bandwidth. In the low frequency range, the pressure fluctuation energy is attributed to the large-scale turbulence in the incident wind. In the high frequency range, small-scale turbulence caused by the building itself introduces additional fluctuation energy so that the amplitudes of the pressure spectra are much larger than those of the wind spectra. It is the small-scale turbulence associated with "delta wing" corner vortices or cylindrical vortices that causes extremely negative pressures in the three taps. The small-scale turbulence may also significantly affect fatigue characteristics of the pressures. The spectral characteristics described here are consistent with those obtained by Eaton and Mayne (1975) on the two-story houses at Aylesbury.

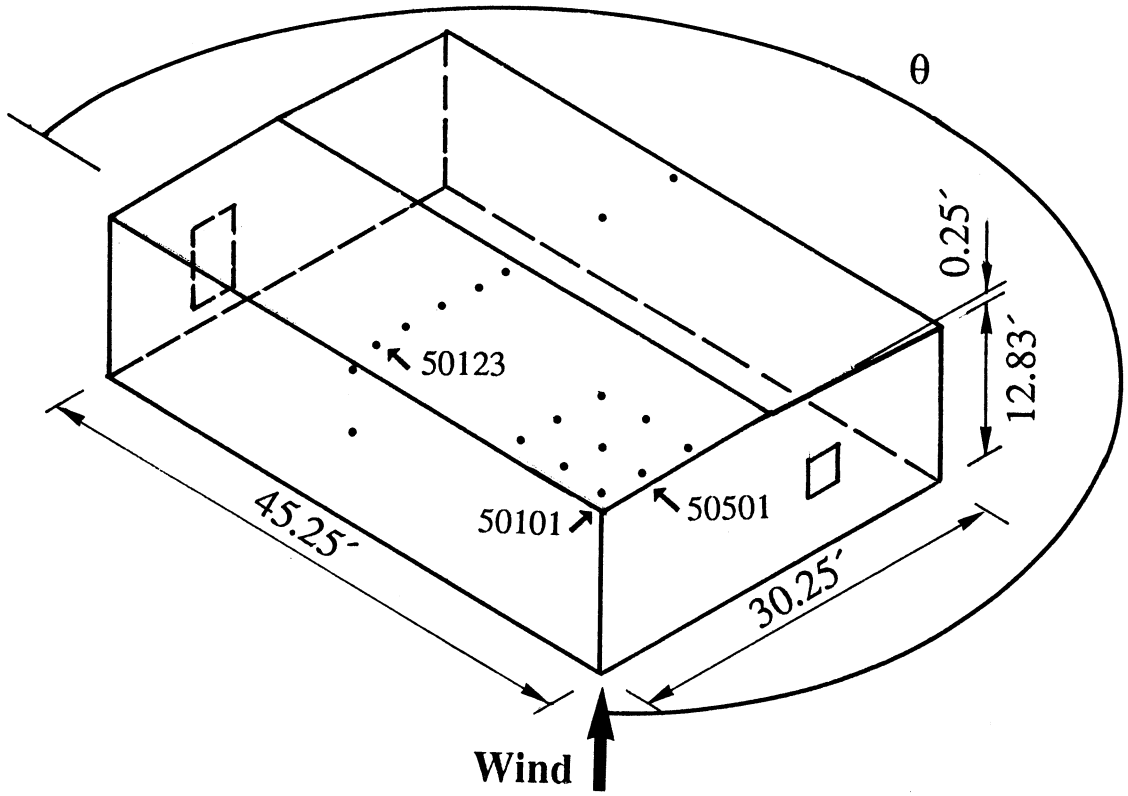

FIG.2.1 TTU BUILDING CONFIGURATION AND TAP LOCATIONS (AFTER MEHTA, 1992)

TABLE 2.1 Pressure Coefficients and Mean Wind Speeds

Tap No. (1)	50123 (2)	50101 (3)	50501 (4)
Mean coefficient	-1.10	-0.63	-2.08
Rms coefficient	0.43	0.44	1.25
Maximum peak coefficient	-0.02	0.50	0.34
Minimum peak coefficient	-4.90	-7.81	-9.00
Mean wind speed (m/s)	9.41	10.12	10.12

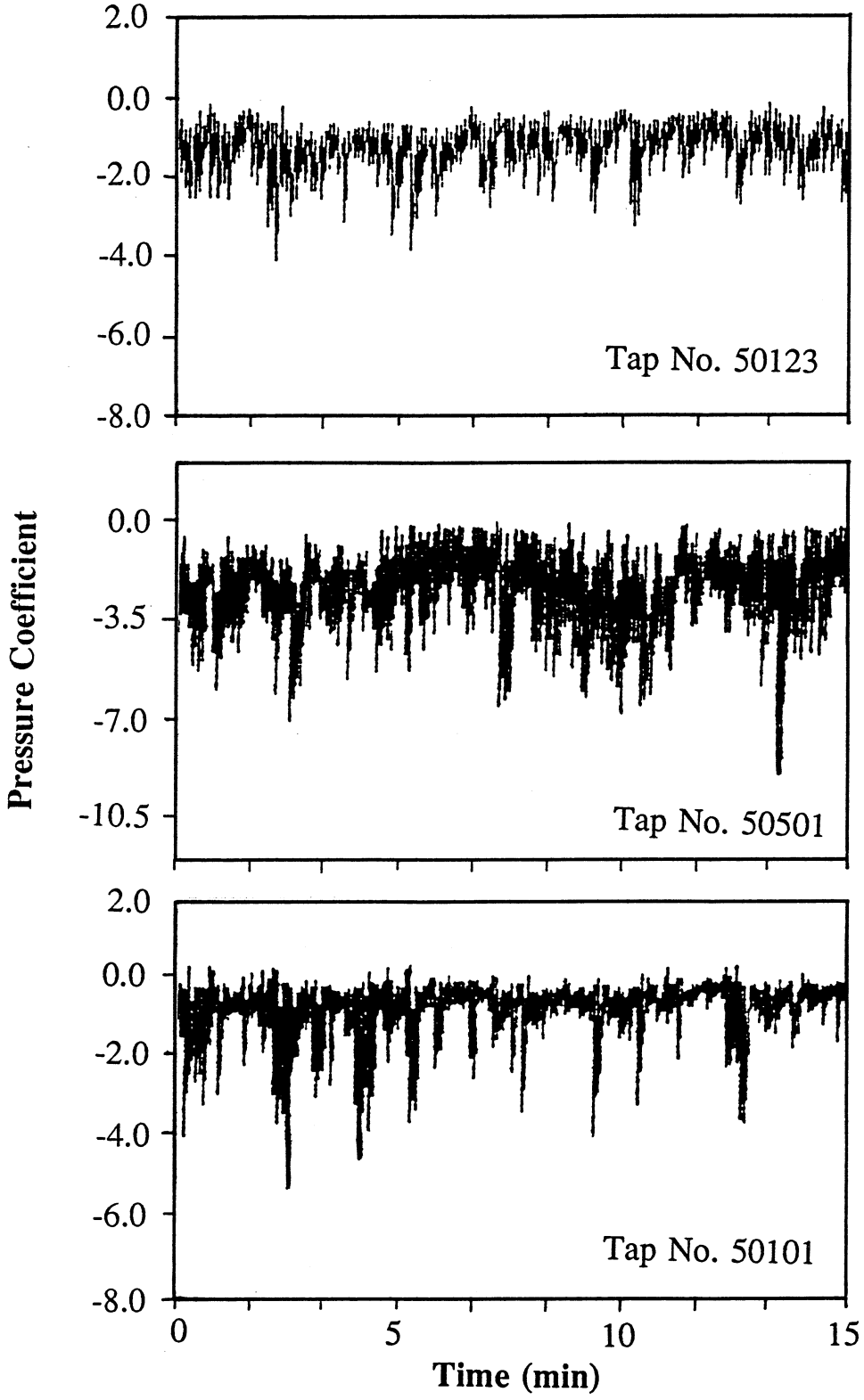

FIG.2.2 TIME HISTORIES OF PRESSURE COEFFICIENTS FOR THREE TAPS (FROM WERFL,TTU)

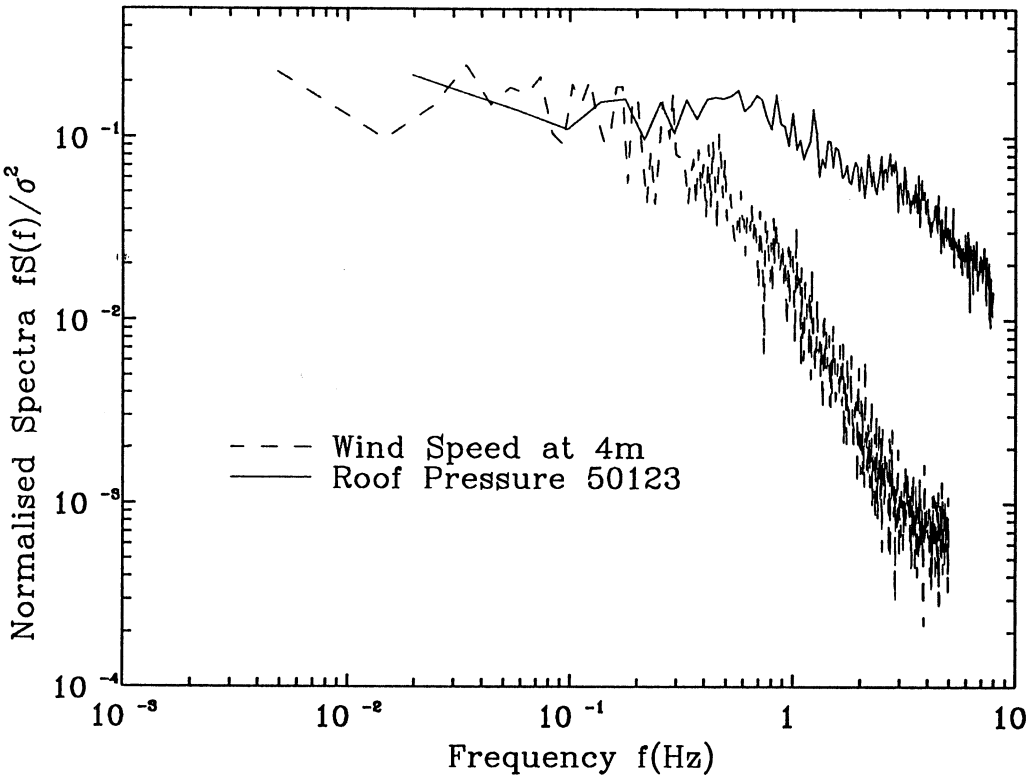

FIG.2.3 WIND SPEED AND PRESSURE SPECTRA FOR TAP 50123

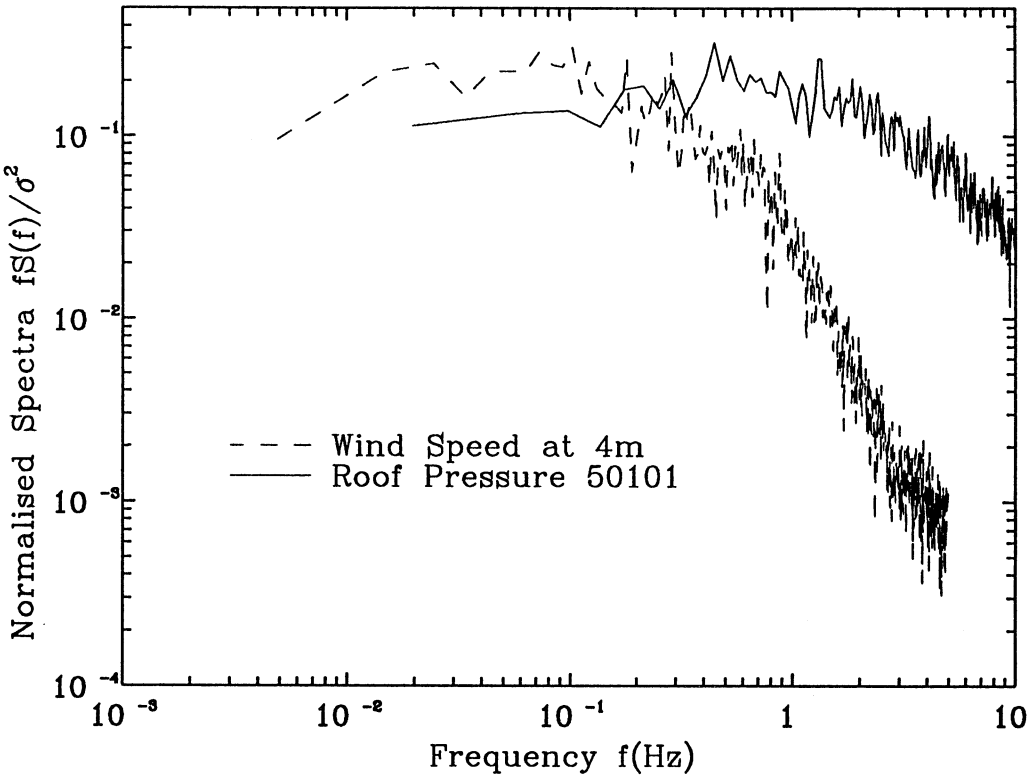

FIG.2.4 WIND SPEED AND PRESSURE SPECTRA FOR TAP 50101

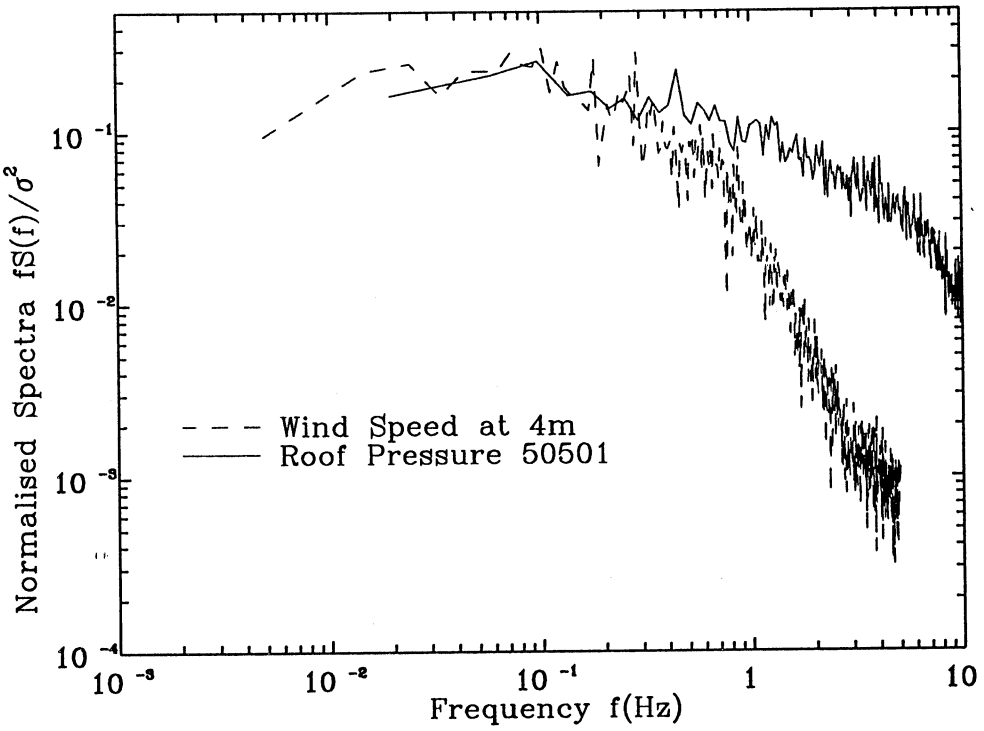

FIG.2.5 WIND SPEED AND PRESSURE SPECTRA FOR TAP 50501

For any stationary random process, a spectrum (i.e. spectral density function) can be defined and the bandwidth of the spectrum can be evaluated by one of two parameters: irregularity factor α or spectral width parameter ε (Lin, 1967; Wirsching and Light, 1980). The irregularity factor α is defined as,

$$\alpha = \frac{m_2}{(m_o m_4)^{1/2}} \tag{2.1}$$

in which m_k is the kth moment of the spectrum (m_o is equal to σ^2) and can be computed from the spectrum S(f).

$$m_k = \int_0^\infty f^k S(f) df \tag{2.2}$$

in which f is the frequency in Hz.

The spectral width parameter ε can then be calculated using the following equation:

$$\varepsilon=(1-\alpha^2)^{1/2} \tag{2.3}$$

The parameters α and ε lie between zero and one. The upper limit $\alpha=1$ or the lower limit $\varepsilon=0$ corresponds to a narrow-band process. When the parameter α approaches zero or the parameter ε approaches one, the random process is called broad-band process.

By using the above equations, the parameters α and ε of spectra of the three pressures are calculated. The parameters are found to be nearly the same for all the three pressures. On the average, the parameter α is 0.24 whilst the parameter ε is 0.97. Therefore, all the three pressures should be regarded as broad-band processes, which result from both the large scale turbulence and the small scale turbulence.

2.3 Probability Analysis of Roof Pressures

It is useful to have a knowledge of probability density functions of roof pressures when one wants to determine cycle count methods and to identify fatigue characteristics of roof pressures. The probability density function is usually expressed in peak factor form. The dimensionless peak factor, g, is defined as

$$g=\frac{p-p_m}{p_{rms}} = \frac{C_p-C_{p_m}}{C_{p_{rms}}} \tag{2.4}$$

in which p is the wind-induced pressure on the tap; p_m and p_{rms} are the mean pressure and the root mean square pressure, respectively; C_p, C_{pm} and C_{prms} are the pressure coefficient, the mean pressure coefficient and the root mean square pressure coefficient, respectively.

Fig. 2.6 shows the probability density function for the tap 50123. The results from three records of 15-minute duration are included in the figure. The standard Gaussian distribution is also plotted. It is obvious that the probability distribution of the tap 50123 is not a Gaussian distribution. There are significant deviations from the Gaussian distribution on both tails of the peak factor. A remarkable number of points are past five standard deviations from the mean, which indicates a much higher probability for the larger negative pressures than a Gaussian distribution would predict. On the other hand, the probability of the larger positive pressures is smaller than that

predicted by a Gaussian process, and the peak of the distribution near zero is shifted slightly to the positive side. This evidence indicates that the pressure under cylindrical vortices could be very negative. Similar observations were reported by Peterka and Cermark (1975) and Stathopoulos (1982).

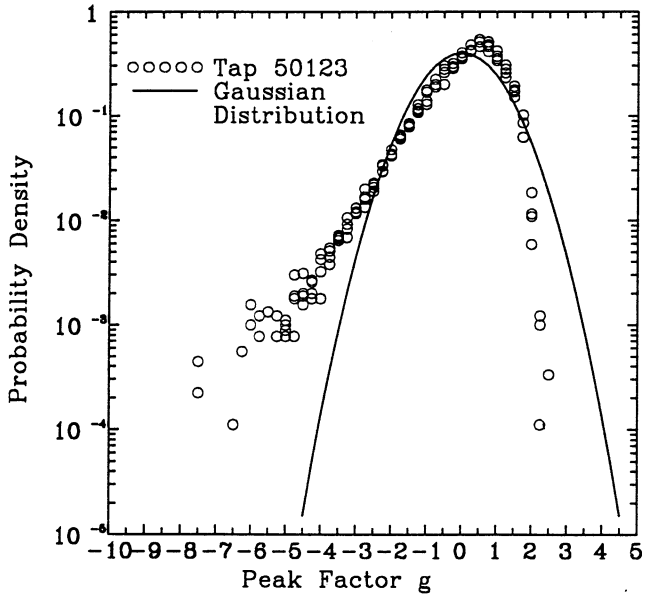

FIG.2.6 COMPARISON OF PROBABILITY DISTRIBUTION OF LOCAL PRESSURE WITH GAUSSIAN DISTRIBUTION---TAP 50123

The most severe deviations from the Gaussian distribution can be found in Fig. 2.7 for the tap 50101, which is located at the upwind corner. The negative peak factors significantly deviated from the Gaussian distribution, and the minimum peak factor was nearly -10. Compared with the tap 50123 shown in Fig. 2.6, the pressure fluctuation on the tap 50101 has a much higher probability in the range of large negative peak factor and in the range around the zero peak factor. These features are attributed to a number of isolated peaks of short duration and high suction, and a large number of fluctuations of small suction around the mean level (see Fig. 2.2).

It is interesting to find that the probability distribution of the pressure fluctuation on the tap 50501 appears to fit the Gaussian distribution well in the negative peak factor region (Fig. 2.8). In the positive peak factor region only a few points exceed a peak factor of 2. Such significant differences of the probability distributions between the taps 50101 and 50501, which are so close to each other, indicate that the pressure distribution over the upwind roof corner is very sensitive to the tap position. The tap 50101 is probably located at the intersection of two "delta-wing" vortices along each windward edge whilst the tap 50501 is only under a single "delta-wing" vortex.

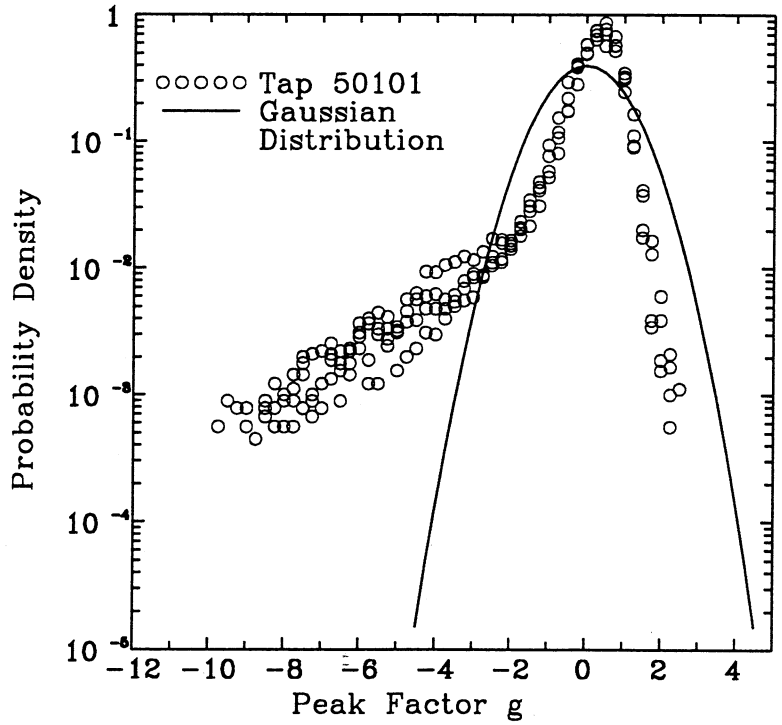

FIG.2.7 COMPARISON OF PROBABILITY DISTRIBUTION OF LOCAL PRESSURE WITH GAUSSIAN DISTRIBUTION---TAP 50101

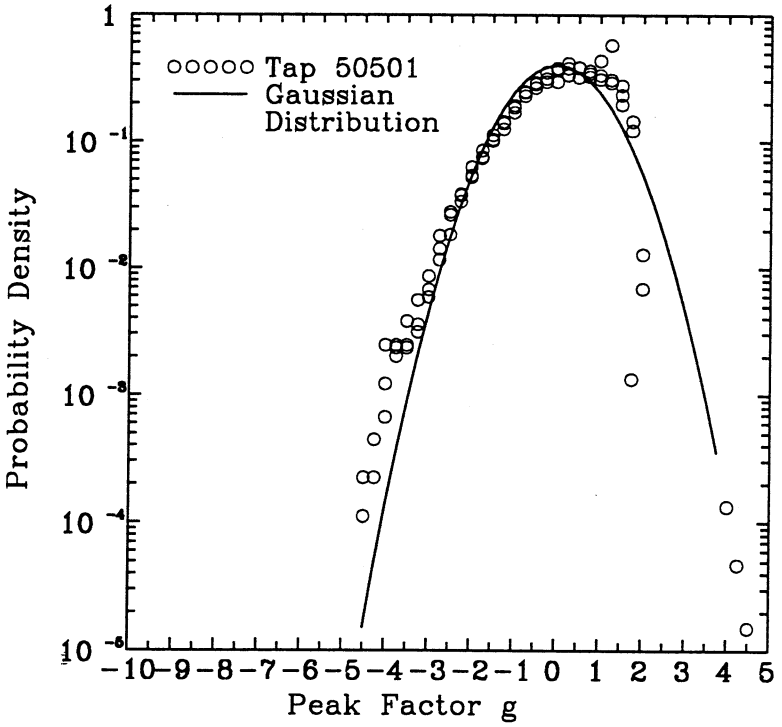

FIG.2.8 COMPARISON OF PROBABILITY DISTRIBUTION OF LOCAL PRESSURE WITH GAUSSIAN DISTRIBUTION---TAP 50501

In view of the preceding discussion, it could be concluded that the probability distributions of the roof pressures of concern are not Gaussian distributions. They are dependent on the tap location and the wind direction.

2.4 Extreme Value Analysis of Roof Pressures

In the existing load cycle distributions, the ranges of load cycles are usually expressed as percentages of the peak load. It is common to simply take the largest peak pressure (absolute value) from a single one-hour record as the peak load for the design purpose. However, the largest peak in the record may be caused by the pressure measurement system itself rather than the real largest peak. Furthermore, Cochran and Cermark (1992) found that the peak coefficients for the taps 50101 and 50501 measured on TTU Building in the field were much higher than those measured in wind tunnels. Therefore, a crosscheck through the extreme value analysis of pressures is desirable.

For each tap of concern, two one-hour consecutive records are available. One hundred independent largest peaks (absolute value) are selected from each one-hour record according to Peterka's criterion (1983). The criterion for selecting independent peaks is that a peak has to be at least 0.05 in peak coefficient away from the adjacent valley. To these one hundred independent peaks a Fisher-Tippet Type 1 (FT1) extreme value distribution is fitted in a manner suggested by Peterka (1983). The results are listed in Table 2.2 for each one-hour record, which include the mode, U, and dispersion, 1/a, of the extreme value distribution for one hundred independent largest peaks, the extreme peak coefficient, C_p^*, the mean extreme peak coefficient, C_p^m, and the single largest peak coefficient, C_p^s.

TABLE 2.2 Results of Extreme Value Analysis of Roof Pressures

Tap No. (1)	50123 Set 1 (2)	50123 Set 2 (3)	50101 Set 1 (4)	50101 Set 2 (5)	50501 Set 1 (6)	50501 Set 2 (7)
U	-3.27	-3.07	-3.65	-4.47	-6.51	-6.29
1/a	-0.32	-0.29	-0.55	-0.51	-0.49	-0.39
C_p^*	-5.18	-4.84	-6.94	-7.52	-9.45	-8.63
C_p^m	-4.92	-4.60	-6.49	-7.09	-9.05	-8.31
C_p^s	-4.69	-4.90	-7.52	-7.81	-9.00	-8.31

in which the extreme peak coefficient and the mean extreme peak coefficient are obtained using the following equations:

$$C_p^* = U + \frac{[1.4 + \ln(100)]}{a} \tag{2.5}$$

$$C_p^m = U + \frac{[0.577 + \ln(100)]}{a} \tag{2.6}$$

It is noted that the ratio of the mean extreme peak coefficient to the corresponding extreme peak coefficient is 0.95 for the tap 50123, 0.94 for the tap 50101 and 0.96 for the tap 50501. In the case of the tap 50501, the single largest peak coefficient, C_p^s, is nearly the same as the mean extreme peak coefficient. In the case of the tap 50101, the single largest peak coefficient is slightly larger than the extreme peak coefficient. It is also found that for all the three taps, when the single largest peak coefficient is approximately equal to the mean extreme peak coefficient, the extreme value distribution of one hundred largest peaks does fit well to the FT1 distribution (see Figs. 2.9 and 2.10). When the single largest peak coefficient is larger than the extreme peak coefficient, the extreme value distribution does not fit well to the FT1 distribution in the range of large negative peak pressure coefficients (see Fig. 2.11).

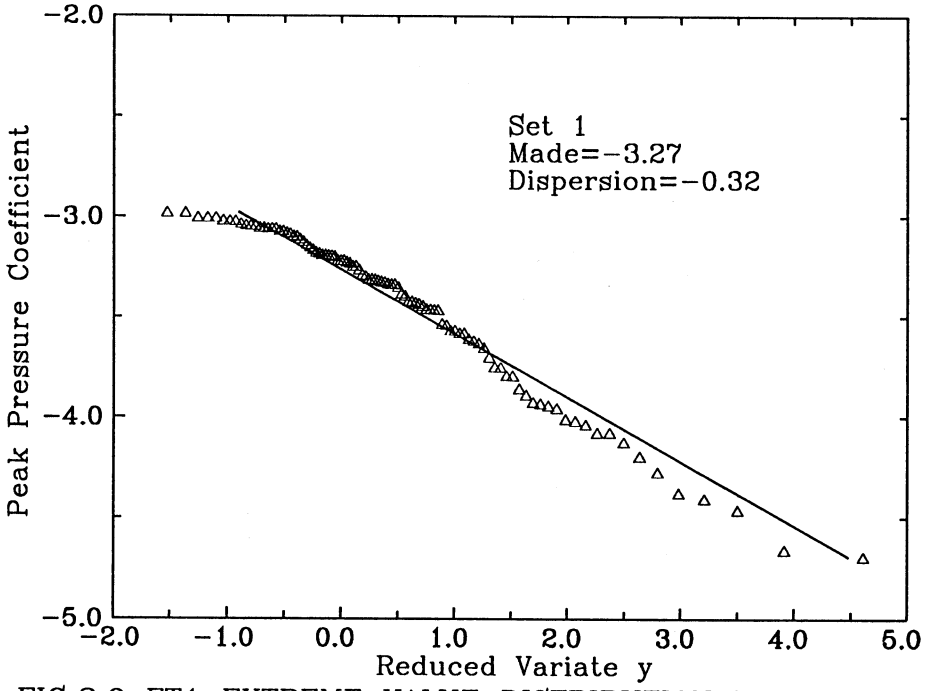

FIG.2.9 FT1 EXTREME VALUE DISTRIBUTION FITTED TO ONE HUNDRED LARGEST PEAKS FOR TAP 50123

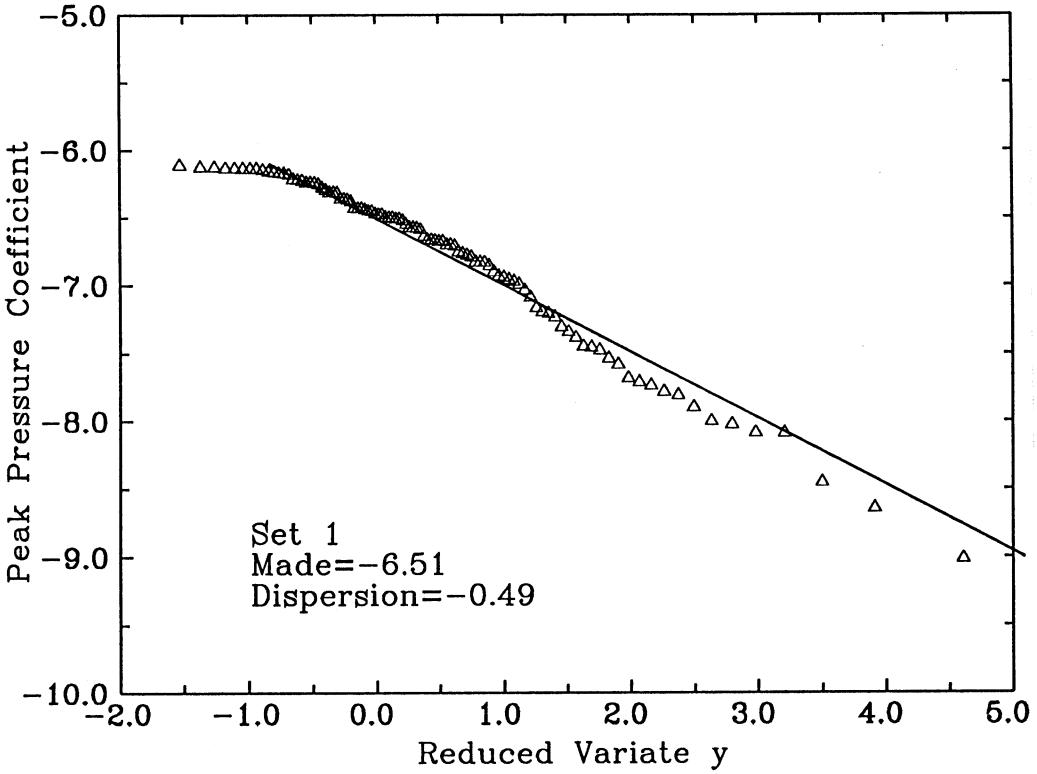

FIG.2.10 FT1 EXTREME VALUE DISTRIBUTION FITTED TO ONE HUNDRED LARGEST PEAKS FOR TAP 50501

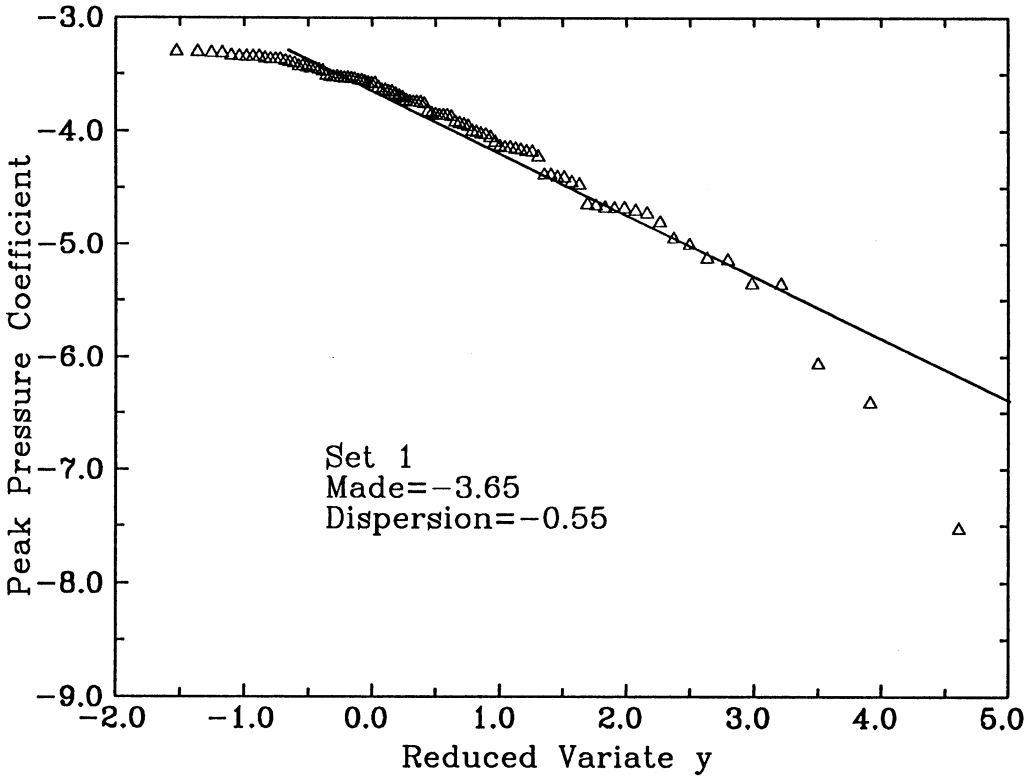

FIG.2.11 FT1 EXTREME VALUE DISTRIBUTION FITTED TO ONE HUNDRED LARGEST PEAKS FOR TAP 50101

The single largest peaks in the pressure records seem to be a real peak. It is therefore decided to use the single largest peak in the two one-hour records as the peak pressure in the later fatigue loading analysis. The expression of the reduced variate, y, in Figs. 2.9 to 2.11 is $a(C_p-U)$ in which C_p represents a peak coefficient from the one hundred largest peak coefficients.

3 FATIGUE CHARACTERISTICS OF ROOF PRESSURES

3.1 Rainflow Count Method

The preceding analyses and results clearly demonstrate that the roof pressure fluctuations concerned here are a broad-band non-Gaussian process. As discussed in Section 1.3, the upcrossing method is not suitable to be employed to count load cycles of such a process. The Committee on Fatigue and Fracture Reliability of the American Society of Civil Engineer (1982) suggest to use the rainflow count method to count load cycles of a broad-band non-Gaussian process. Dowling (1972) conducted many experiments and provided strong supporting evidence that the rainflow count method is superior to the other count method, such as peak method, level crossing method and range-pair method. The rainflow count method has been used by Wirsching and Light (1980), Chaudhury and Dover (1985) and many others to count cycles of sea wave loads acting on the offshore platforms. It has also been used by Lambert et al (1988) and Jancauskas et al (1990) to count cycles of wind-induced stress response or pressure. A full definition of the rainflow method can be found in Dowling and Socie (1982).

The rainflow count method was first proposed by Matsuishi and Endo (1968). It can identify load cycles which are compatible with a large quantity of material or structure fatigue data from constant-amplitude fatigue tests. This method is particularly useful for low-cycle fatigue, as it can identify cycles as closed hysteresis loops and provide the mean cycle level for each cycle. However, the rainflow method gives no information about original load or stress cycle sequence, which may have a pronounced influence on fatigue life estimate of some materials or structures. It is also extremely difficult to formulate the probability equations for cycle ranges and cycle mean levels obtained through the rainflow method. Although some attempt has been made to find rainflow range density functions (Bishop, 1990), the rainflow method is usually employed in conjunction with computational technology.

3.2 Number of Cycles

A Fortran program executing the rainflow count method has been written and used to count load cycles for all roof pressure records of a 15-minute duration. Hysteresis thresholds, or dead bands, are employed when processing the time-histories of the pressures. A few of the small positive peaks in the pressure time-histories are filtered. The number of cycles with time is shown in Figs. 3.1 to 3.3 for the three taps, respectively. Different hysteresis thresholds are considered. It is clear that the number of cycles increases with time for all the thresholds of concern. The relationship between the number of cycles and the time is approximately linear, particularly in the cases of the taps 50123 and 50501. The number of cycles reduces most significantly when the hysteresis threshold increases from 0.1 to 0.2 of the single largest peak coefficient, C_p^s.

It is noted that the number of cycles is different among the three taps. At the same threshold, the tap 50501 has the largest number of cycles, and the tap 50101 has the smallest number of cycles. The number of cycles per hour, corresponding a threshold of 0.05 of the single largest peak coefficient, is 3166 cycles for the tap 50123, 2291 cycles for the tap 50101 and 6642 cycles for the tap 50501.

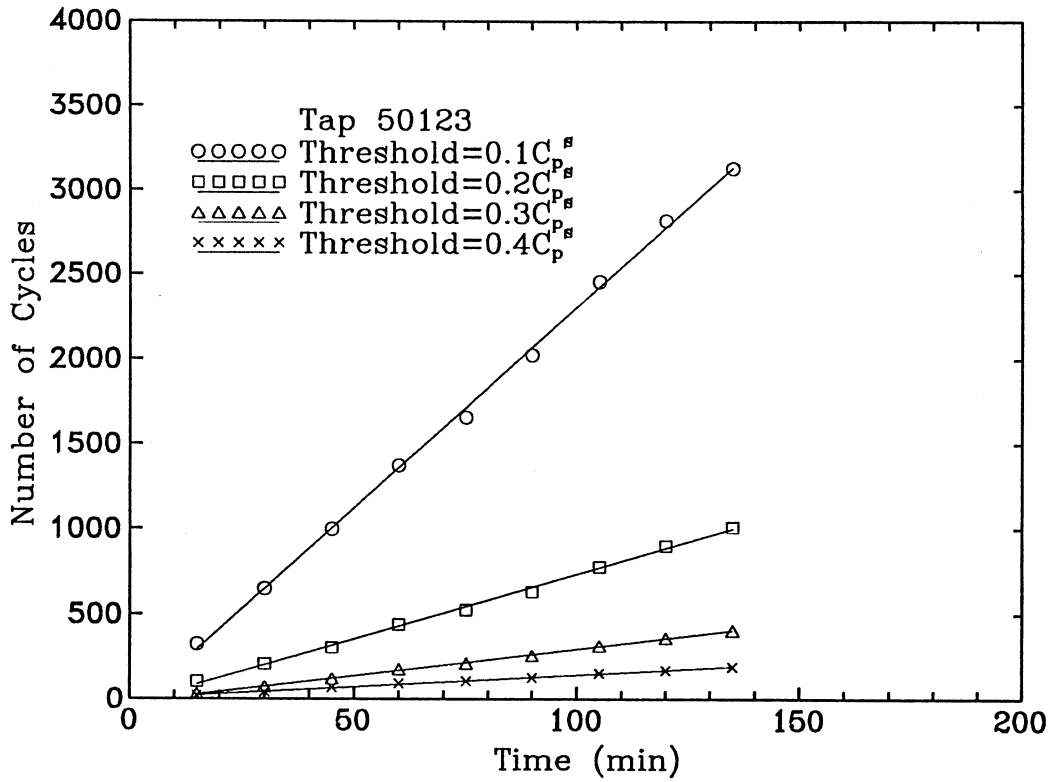

FIG.3.1 THE RELATIONSHIP BETWEEN THE NUMBER OF CYCLES AND TIME FOR TAP 50123

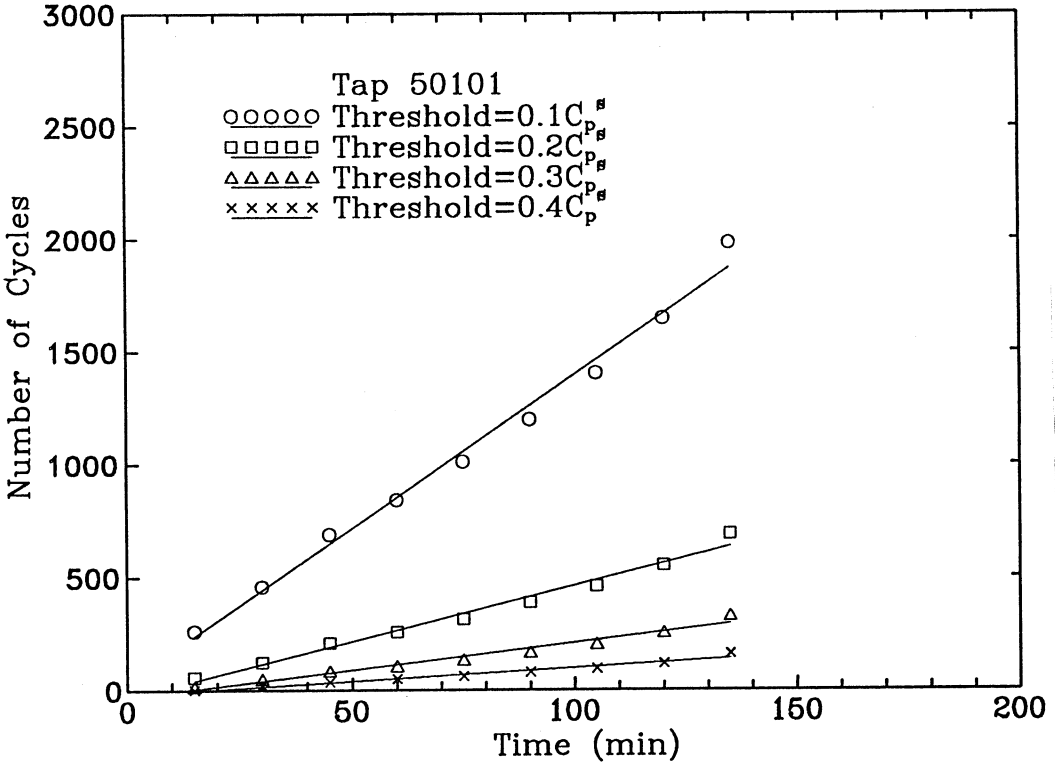

FIG.3.2 THE RELATIONSHIP BETWEEN THE NUMBER OF CYCLES AND TIME FOR TAP 50101

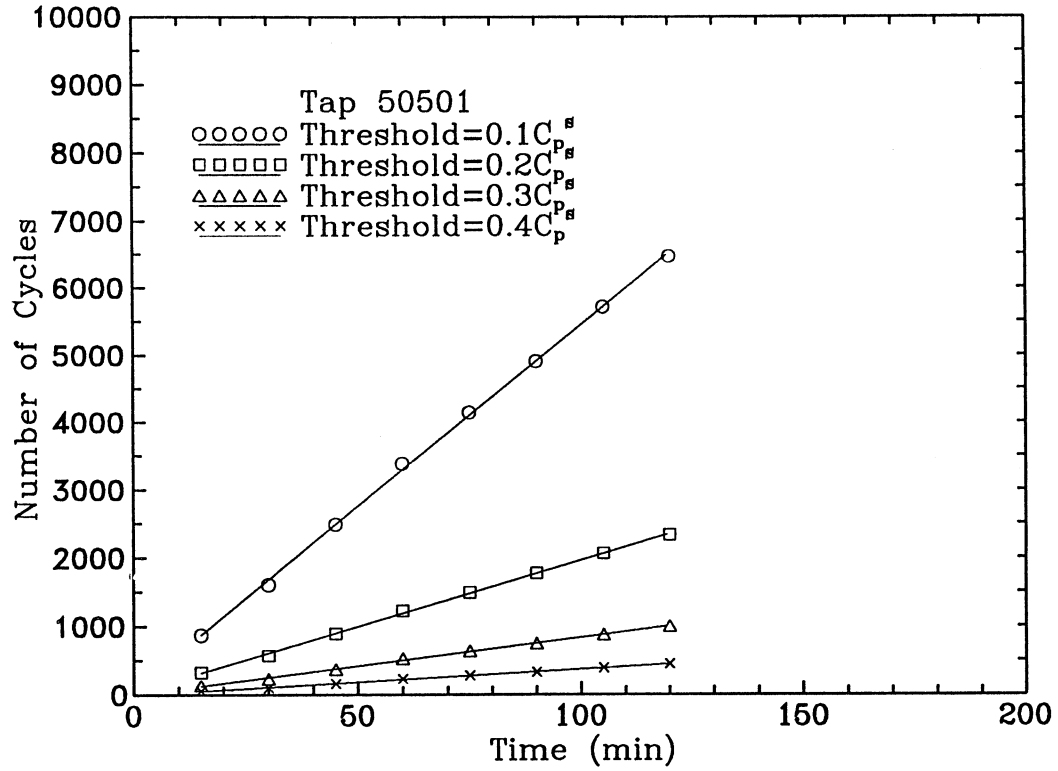

FIG.3.3 THE RELATIONSHIP BETWEEN THE NUMBER OF CYCLES AND TIME FOR TAP 50501

Another important feature is the relationship between the wind speed and the number of cycles. Although it could not be demonstrated in this study because of the limitation of the available data, the similarity equation associated with the Strouhal number or reduced velocity indicates that the number of cycle is proportional to the wind speed. This linear relationship has been used by Lynn and Stathopoulos (1985) and Jancauskas et al.(1990).

As listed in Table 2.1, the mean wind speed at the roof height of the TTU building is 9.41 m/s for the tap 50123, and 10.12 m/s for the taps 50101 and 50501. After considering the linear relationship, the cycle number per hour per wind speed (m/s), $\bar{n}$, is 336 cycles for the tap 50123, 225 cycles for the tap 50101, and 652 cycles for the tap 50501 at a threshold of 0.05 of the individual single largest peak coefficient.

3.3 Cycle Histogram

A three dimensional cycle histogram can be used to describe the load cycle distribution of the pressure itself over both cycle ranges and cycle mean levels. Figs. 3.4 to 3.6 display the cycle histograms for the three pressures, respectively. Each histogram is achieved by averaging eight or nine similar histograms obtained from 15-minute records. The range and mean level of cycles are expressed as percentage of the single largest peak coefficient. The number in each cell is the proportion of the cycle number in this cell to the total cycle number. The hysteresis threshold is still 0.05 of the single largest peak coefficient. The cycle histogram defined here, together with information on long-term wind climate, could provide the required total load cycle distribution.

It is noted from Figs. 3.4 to 3.6 that there are considerable differences in the three cycle histograms. Compared with the other two taps, the load cycles of the tap 50101 are much concentrated on the cells of the lowest cycle mean level. In the area of high-level ranges or means of cycles, a few blank cells exist. The cycle histogram of the tap 50123 is much smoother than that of the tap 50101, and most cycles are concentrated on the area of low cycle ranges. The proportion of cycle number of the tap 50501 is most uniformly distributed compared with the other two taps, which means there are a quite few of cycles of high ranges or high mean levels in the tap 50501. These features are consistent with the different probability distributions of the peak factor discussed in Section 2.3. Nevertheless, more research is required to find the relationship between the probability distribution of the peak factor and the load cycle histogram of the pressure.

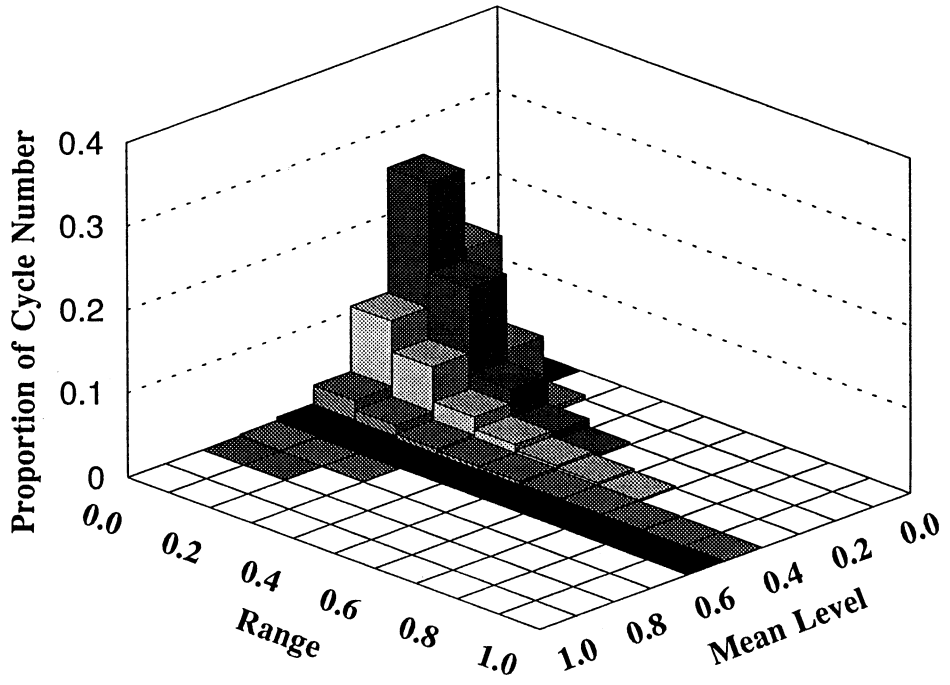

FIG.3.4 CYCLE HISTOGRAM OF TAP 50123

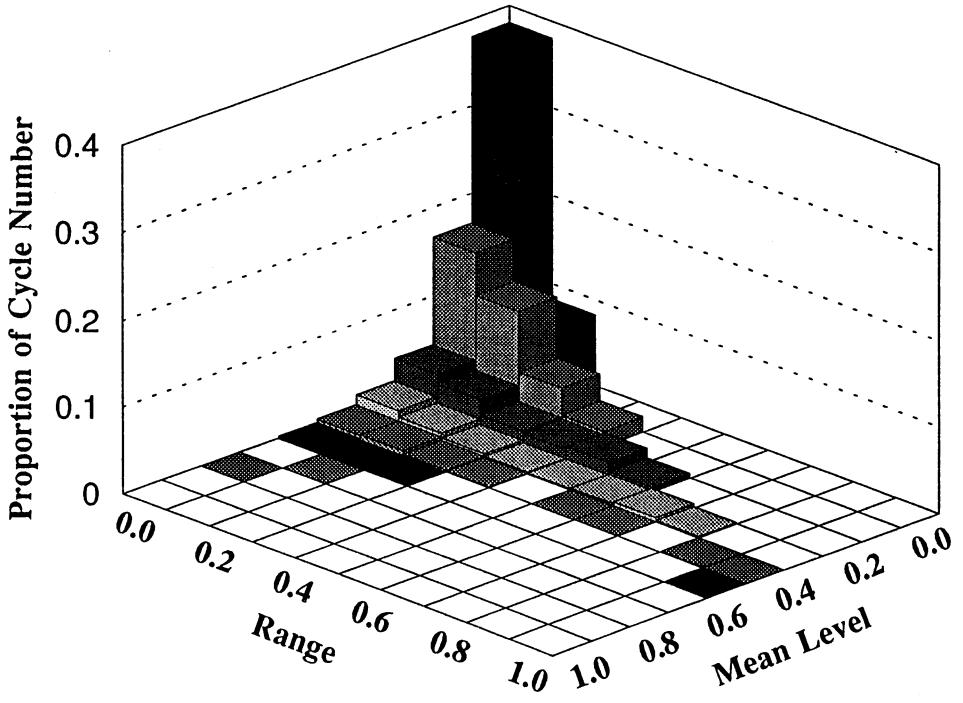

FIG.3.5 CYCLE HISTOGRAM OF TAP 50101

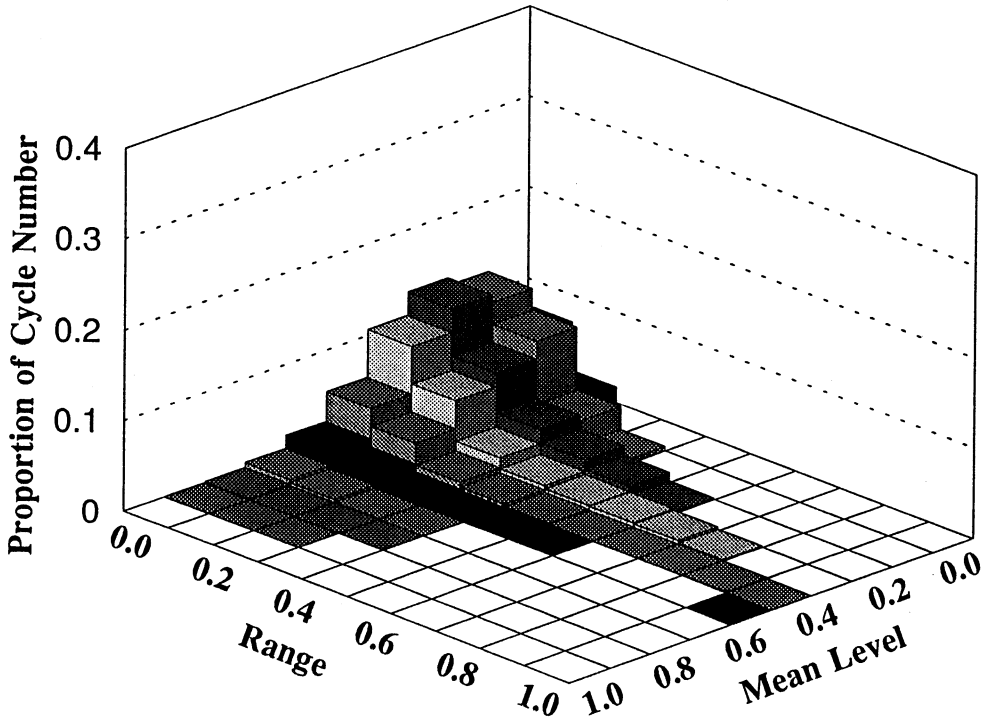

FIG.3.6 CYCLE HISTOGRAM OF TAP 50501

Two dimensional cycle distributions over cycle ranges only or over cycle mean levels only are plotted in Figs. 3.7 and 3.8, respectively. In these individual distributions, the proportions of cycles in each cell of the joint cycle histogram have been divided by the cell width. It can be seen from these figures that all the three taps have nearly the same cycle distributions over cycle ranges, but the distributions over cycle mean levels are different. It is desirable to find the relationship between the two individual cycle distributions and the joint cycle histogram.

4 FATIGUE LOADING ON ROOF CLADDING

4.1 Wind Climate

Fatigue damage to the metal roof of low-rise buildings actually accumulates from storm to storm and from hour to hour in the regions dominated by large scale weather systems, and it also accumulates from cyclone to cyclone during the design life of roof cladding in cyclone regions. Therefore, a knowledge of wind climate is required.

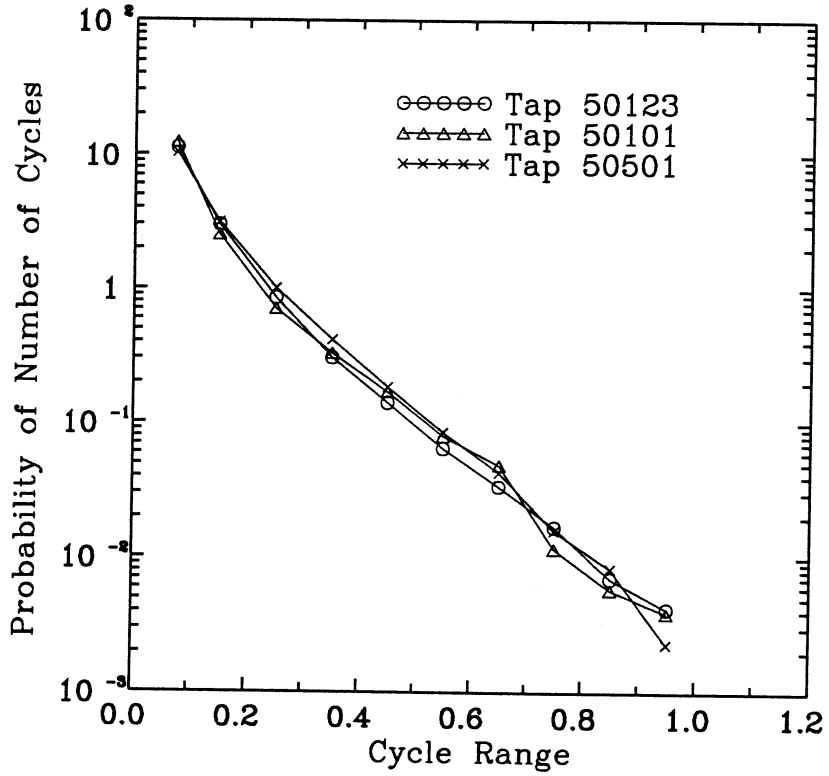

FIG.3.7 INDIVIDUAL CYCLE DISTRIBUTIONS OVER CYCLE RANGE

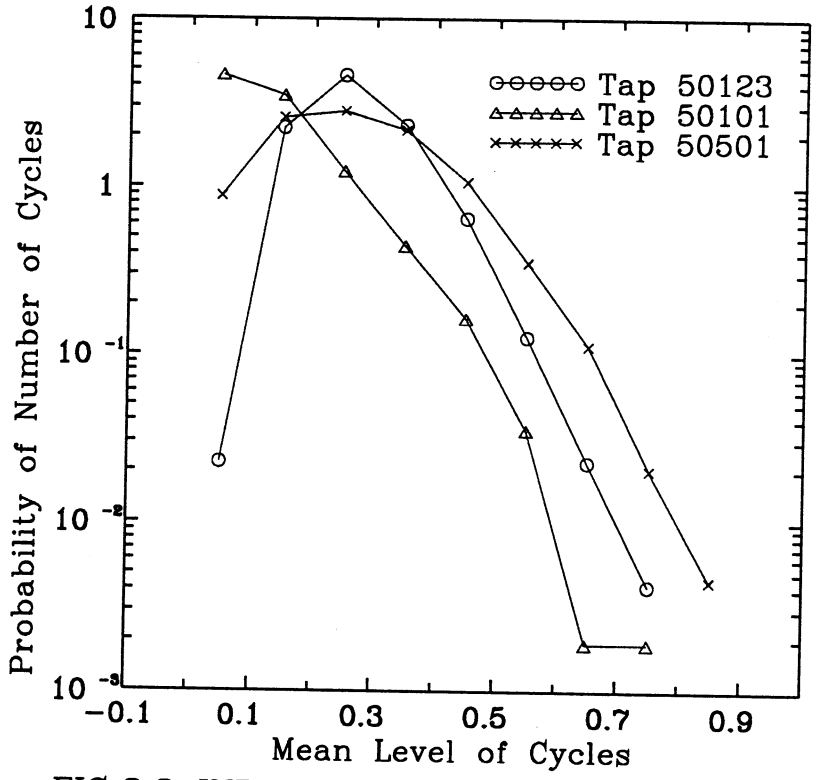

FIG.3.8 INDIVIDUAL CYCLE DISTRIBUTIONS OVER MEAN LEVEL OF CYCLES

In Region A, which covers most of Australia, dominant wind gusts are either gales associated with large scale weather systems or thunderstorm downdraughts (Holmes et al, 1990). Strong gusts generated by thunderstorm downdraughts are extremely unstable (non-stationary and transient) and the velocity profiles above the ground are not adjusted to the roughness of the underlying terrain (Holmes, 1993). Therefore, the cycle histograms obtained using the data measured on the TTU Building are not suitable for the case of thunderstorm downdraughts. The fatigue problem caused by thunderstorm downdraughts has to be left for further research.

Davenport (1967) has shown that for the wind region dominated by large scale weather systems, the parent distribution of wind speeds is well modelled empirically by the Weibull distribution. Wayne (1979) has also shown that the Fisher-Tippett Type 1 (FT1) distribution could well represent the extreme value distribution of the wind in such regions (i.e., temperate regions). Dorman (1982, 1983) used the FT1 distribution to fit the Australia field data. A mode of 29.2 (m/s) and a dispersion of 3.0 (m/s) are used in Australian Wind Loading Code (SAA, 1989) to determine the design wind speeds for Region A.

In this study, the Weibull distribution is used to model the probability distribution of hourly mean wind speeds, V, in temperate regions. The probability density function of the Weibull distribution is

$$p(V)=ckV^{k-1}\exp(-cV^{k}) \tag{4.1}$$

A value of k of 2.0 is used in the computation but the sensitivity to k is examined. The parameter c is determined by the extreme hourly mean wind speed, V_m, associated with a certain return period and design life of roof cladding. For instance, it is assumed that the extreme hourly mean wind speed with a return period of 50 years corresponds to a value of p(V) of 2.28 $\times 10^{-6}$ for a 50-year design life of roof cladding.

The extreme hourly mean wind speeds are determined by Australia Wind Loading Code (SAA, 1989) in terms of the extreme gust wind speeds and the terrain-height multipliers. The extreme gust wind speeds in Region A with respect to certain return period are given by Holmes et al (1990),

$$V_p=29.2+3.0LnR \tag{4.2}$$

in which R is a return period in years, and V_p is the extreme gust wind

speed.

In Regions C and D, the extreme gust wind speeds specified in Australian Wind Loading Code (SAA, 1989) are based on the occurrence of tropical cyclones only. A tropical cyclone is defined as an isobarically closed tropical low pressure system producing a sustained strong wind of at least 17 m/s ten-minute mean speed. Gomes and Vickery (1976) used Monte Carlo simulation technique to simulate tropical cyclones. They found that the probability distribution of extreme gust speeds of the simulated cyclones could be well described by the FT1 distribution. That is

$$P(V_p)=\exp[-\exp(-y)];\quad y=a(V_p-U) \tag{4.3}$$

The corresponding probability density function is

$$p(V_p)=a\exp(-y)\exp[-\exp(-y)] \tag{4.4}$$

Although Dorman (1983) has shown that the Monte Carlo simulation method may not be a reliable tool for determining extreme gust wind speeds in tropical cyclones, the FT1 distribution was still used by Dorman (1984) to fit the field data of wind speed in tropical cyclones. The Australian Wind Loading Code (SAA 1989) recommends the following equation to determine extreme gust wind speeds in Region C (Holmes et al, 1990).

$$V_p=26+6.4LnR \tag{4.5}$$

The following equation is used to determine extreme gust wind speeds in Region D.

$$V_p=23+9.0LnR \tag{4.6}$$

Besides extreme gust wind speeds, another important parameter is the average annual occurrence of tropical cyclones, n_o. In terms of statistics of tropical cyclones during July 1960 to June 1975, Southern (1978) showed that for Onslow-Port hedland region (Region D), the average annual occurrence was about 2.0 (within 5^0 latitude longitude square), and it was about 1.6 for Darwin area (Region C) and about 1.0 for Mackey area (Region C). To be compatible with the Australian Wind Loading Code, it is decided to use 2.0 for Region D and 1.6 for Region C. By using the FT1 probability density function and the average annual tropical cyclone occurrence, the frequency histogram of cyclones could be obtained for a given wind return

period and design life of roof cladding. Fig. 4.1 shows the frequency histogram of cyclones in Region C for a 50-year return period wind over a 50-year design life. It can be seen that the peak gust wind speeds of most cyclones are below 35 m/s and above 22 m/s whilst the cyclone of a 50-year return period gust wind speed occurs only once in the 50-year design life.

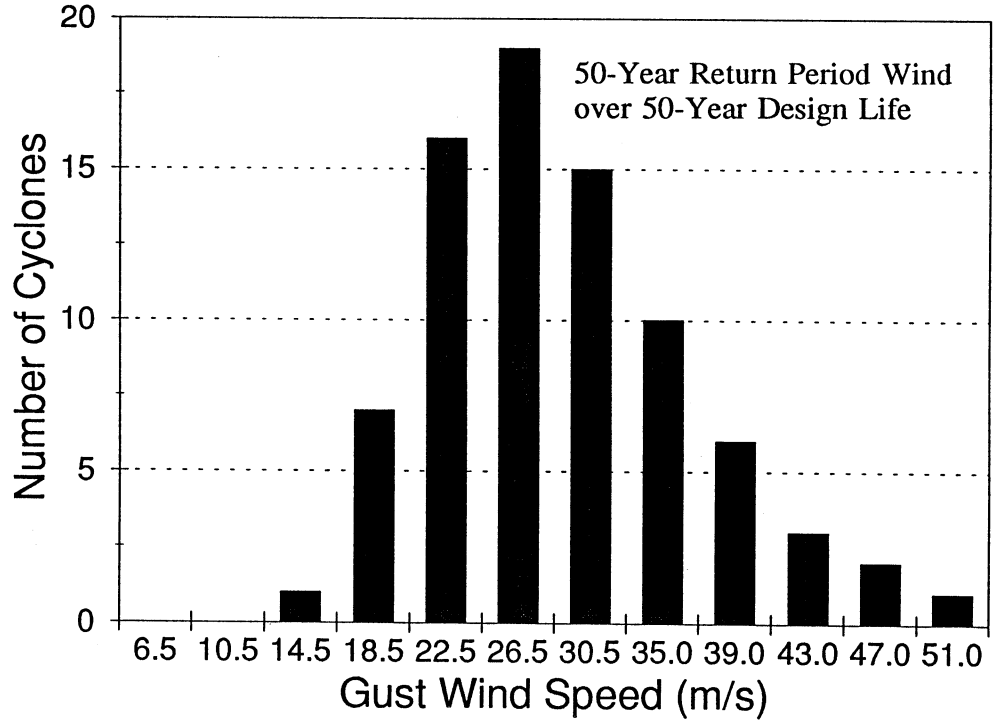

FIG.4.1 FREQUENCY HISTOGRAM OF CYCLONES IN REGION C

Region B in Australia is a mixed region in which both tropical cyclones and thunderstorm downdraughts are critical. No information is available to the author on roof pressures associated with thunderstorm downdraughts so that the corresponding fatigue loading analysis could not be performed here.

4.2 Computation of Fatigue Loading

As to fatigue loading on roof cladding in Region A dominated by large scale weather systems, fatigue loading is accumulated from hour to hour. For a given hourly mean wind speed, V_i, the corresponding number of cycles, N_i, in the design life of roof cladding is

$$N_i=\bar{n}V_i\, p(V_i)(\Delta V)T_R \tag{4.7}$$

in which $\bar{n}$ is the number of cycles per hour per mean wind speed (m/s), as given in Section 3.2; $p(V_i)$ is the probability of the hourly mean wind speed, V_i, determined by the wind return period R and the design life, as given in Section 4.1; ΔV is the cell width in the probability density function of the hourly mean wind speed related to the computation iteration; T_R is the design life in hours (8760 hours per year).

The distribution of the cycles, N_i, over both cycle ranges and cycle mean levels is given by the matrix $[\mathbf{N_i}]$.

$$[N_i]=N_i\ [H_i] \tag{4.8}$$

in which the matrix $[\mathbf{H_i}]$ is the cycle histogram given in Section 3.3 and the subscript i is used to identify range and mean level of cycles, which are now expressed as percentage of the wind pressure, $1/2C_p{}^s\rho V_i^2$.

Let the matrix $[\mathbf{N_1}]$ corresponds to the design wind pressure $1/2C_p{}^s\rho V_m{}^2$ (V_m is the design hourly mean wind speed corresponding to the design gust wind speed V_p), and let the threshold of cycle ranges in all the matrix **[Ni]** be 0.05 of the design wind pressure. The summation of the matrix **[Ni]** then gives the total load cycle distribution of the designated tap for the given wind return period and the design life.

$$[N]=\sum_{i=1}^{J}[N_i] \tag{4.9}$$

It is apparent that the largest cycle ranges in the matrix $[N_{J+1}]$ and the subsequent matrices are below 0.05 of the design wind pressure, and these matrices are therefore ignored.

For the total load cycle distributions in Regions C and D, the number of cycles should be accumulated from cyclone to cyclone. Cyclones experienced by a particular structure may have different central pressures, radius to maximum winds, forward speeds of the eyes and other meteorological factors. Therefore, the wind speed, wind direction and wind duration for the particular structure are variable from cyclone to cyclone. Ideally, a set of load cycle histograms, as given in Section 3.3, should be developed with respect to different wind directions, and Monte Carlo simulation technique may be used to generate a set of cyclones. The fatigue loading generated by each cyclone is calculated and then summed. However, this ideal procedure would involve many cyclone parameters which are still open to question now. In

consideration of the uncertain level of fatigue life estimated by Miner's rule, it is rational to use a conservatively simplified procedure to determine fatigue loading in tropical cyclone regions.

Jancauskas et al (1990) developed a set of load cycle histograms for the pressure at the roof corner of a low building in terms of wind tunnel model tests. They also provided a design cyclone with the typical central pressure, radius to the maximum wind and forward speed of the eye. It is found from their results that for the design cyclone of a 5-hour duration, significant fatigue loading appeared only in two or three hours when the corner pressure was under stronger wind speeds and worse wind directions. Therefore, it is decided to disregard effects of the variations of wind speed and wind direction during a cyclone, and to locate the strongest wind of a 2- or 3-hour duration at the worst location of the roof pressure. Such a simplification provides a commercial prospect for determining wind-induced fatigue loading on structures in terms of wind tunnel model tests.

For a given frequency histogram of cyclones as discussed in Section 4.1, the following equation has been derived to calculate the total load cycle distribution of the pressure in Regions C and D.

$$[N]=\sum_{i=1}^{J} \bar{n} V_{ci} M_{ci} T_h [H_i] \qquad (4.10)$$

in which M_{ci} is the number of the cyclones with an hourly mean wind speed of V_{ci}; T_h is the effective duration of each cyclone (two or three hours). V_{ci} and M_{ci} can be determined from the frequency histogram of cyclones (see Fig. 4.1) and terrain-height multipliers. The principle of the summation of fatigue loading from i=1 to J is the same as that used for Region A.

4.3 Total Load Cycle Distributions

Figs. 4.2 to 4.4 show the total load cycle distributions of the three taps in Region C, respectively. Both cycle ranges and mean levels are expressed as percentage of the design wind pressures which is equal to $1/2\rho V_m^2$ multiplied by the individual single largest peak coefficient. The design hourly mean wind speed, V_m, is calculated based on the design gust wind speed of 51 m/s, a gust wind speed height multiplier and an hourly mean wind speed height multiplier for a terrain of category 2, which are specified in the Australian Wind Loading Code (SAA, 1989). The effective duration of each cyclone is two hours and the design life is 50 years.

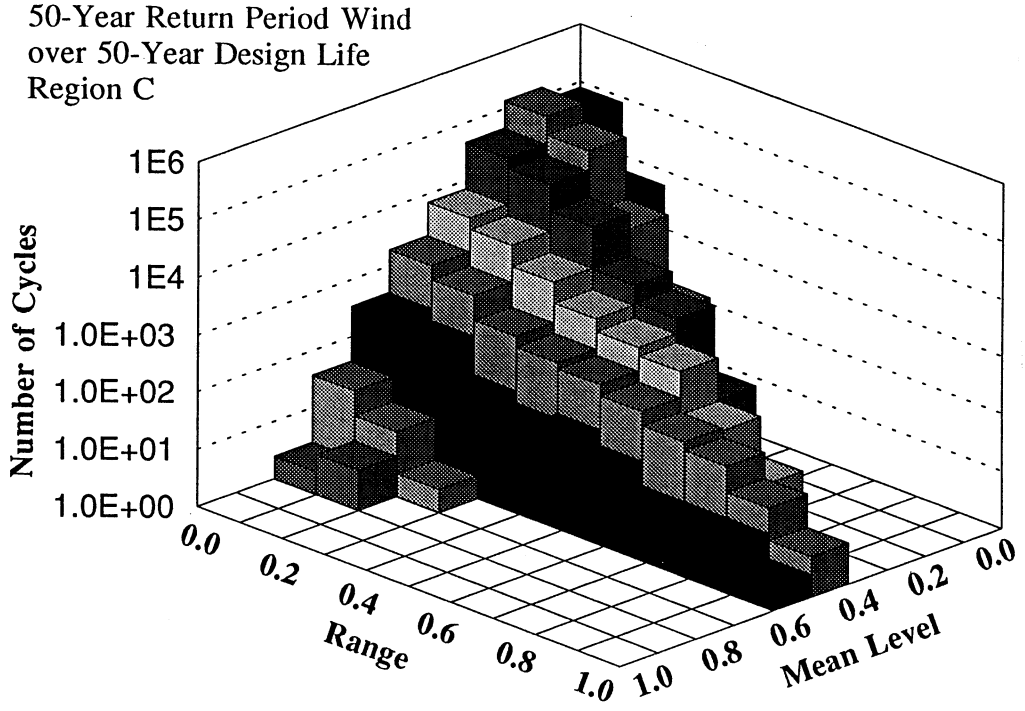

FIG.4.2 TOTAL LOAD CYCLE DISTRIBUTION OF TAP 50123

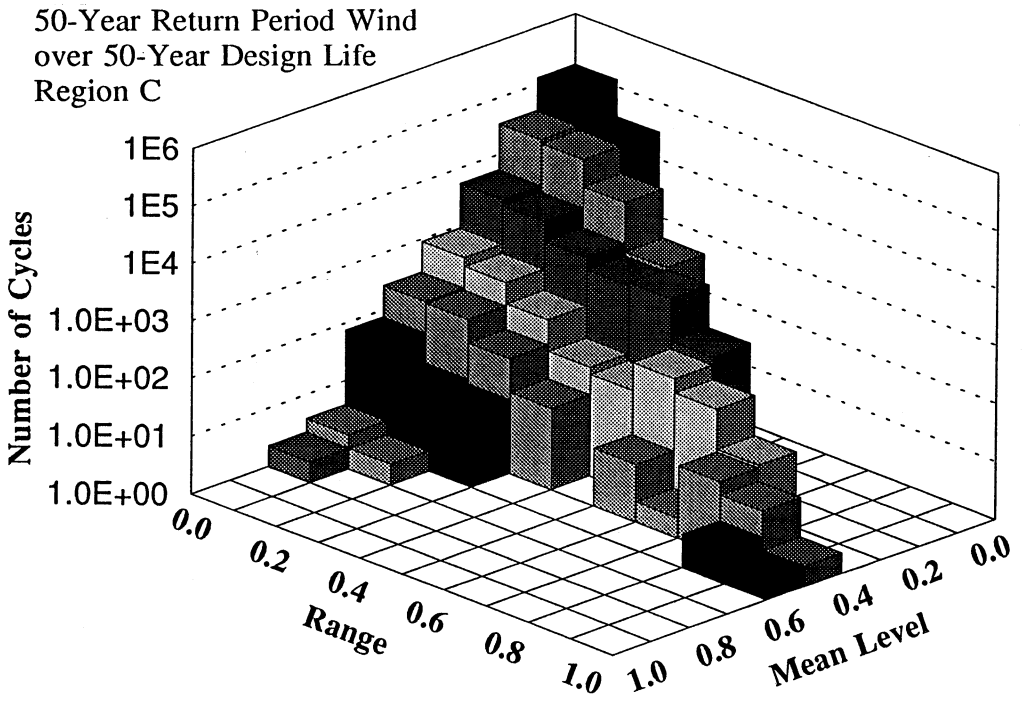

FIG.4.3 TOTAL LOAD CYCLE DISTRIBUTION OF TAP 50101

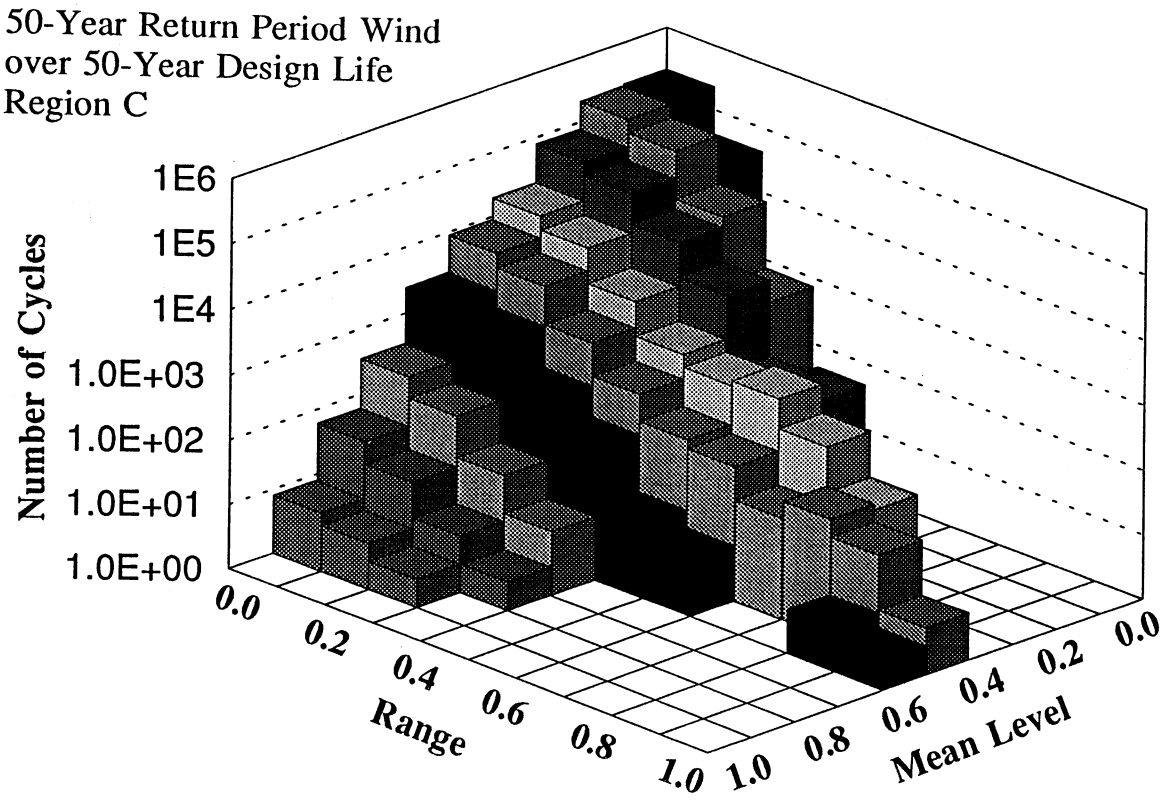

FIG.4.4 TOTAL LOAD CYCLE DISTRIBUTION OF TAP 50501

The common feature for all the three taps is that there is a large number of cycles in the area of both low cycle ranges and low cycle mean levels. As cycle ranges or cycle mean levels become larger, the number of cycles becomes less. Compared with the corresponding cycle histograms as shown in Figs. 3.4 to 3.6, the total load cycle distributions contain more cycles and less blank cells. Due to the accumulation of cyclones, more cycles distribute in the area of low cycle mean levels. It is also seen that the total number of cycles for the tap 50501 is much larger than that for the tap 50101 because the unit cycle number, $\bar{n}$, is much larger in the tap 50501.

Effects of wind regions on total load cycle distributions are shown in Figs. 4.5 to 4.7 in terms of the tap 50501 with a 1000-year return period wind over a 50-year design life of roof cladding. The frequency histogram of cyclones

in this case is assumed to be the same as that shown in Fig. 4.1 except that the gust wind speeds in Fig. 4.1 are replaced by those corresponding to the 1000-year wind return period. The general feature of the three figures is nearly the same, but the total number of cycles is much larger in Region A than those in Region C or D. The reason is that the total load cycle distribution in Region A is accumulated from hour to hour whilst those for Region C or D are accumulated from a few cyclones. The other reason is that for the same wind return period and the same tap, the design wind pressure in Region A is the smallest. Therefore, the same hysteresis threshold of 0.05 of the design wind pressure would lead to a low cut-off of cycles for Region A. The later reason also explains why the number of cycles and the cycle distribution for Region D are nearly the same as those for Region C even though the cyclone occurrence rate, n_o, is higher in Region D than in Region C.

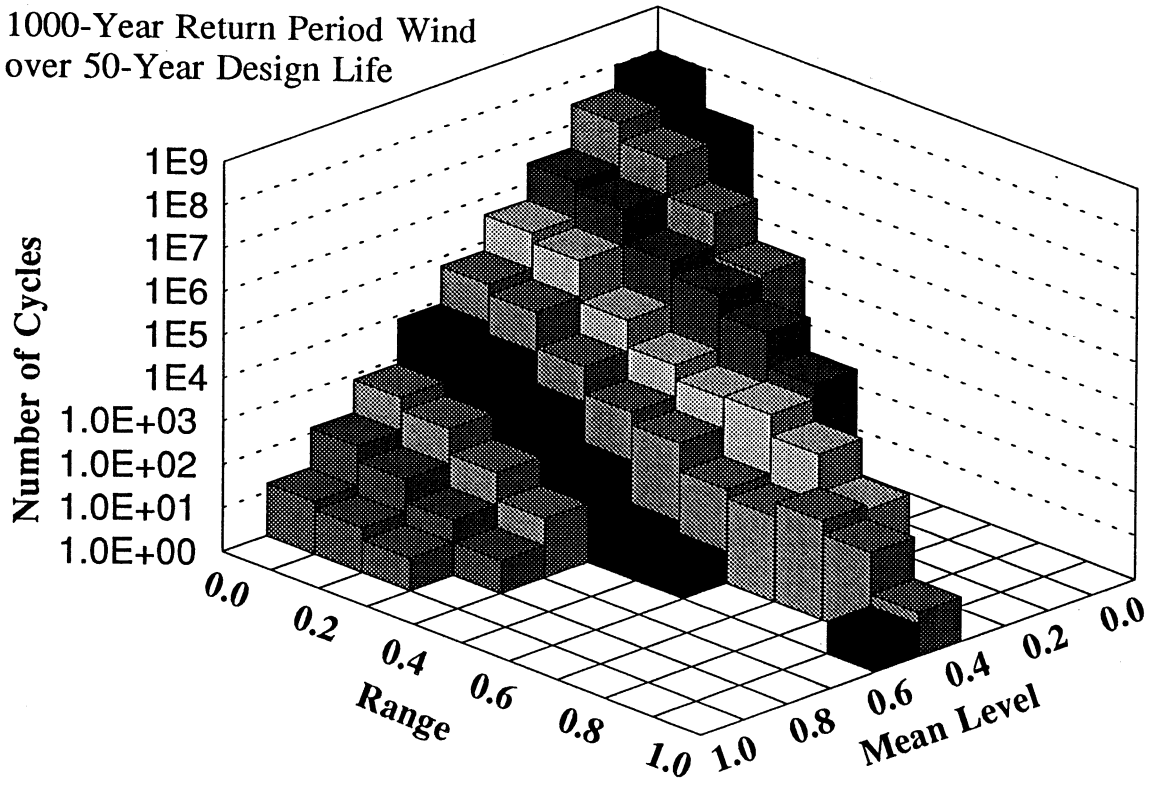

FIG.4.5 TOTAL LOAD CYCLE DISTRIBUTION OF TAP 50501 IN REGION A

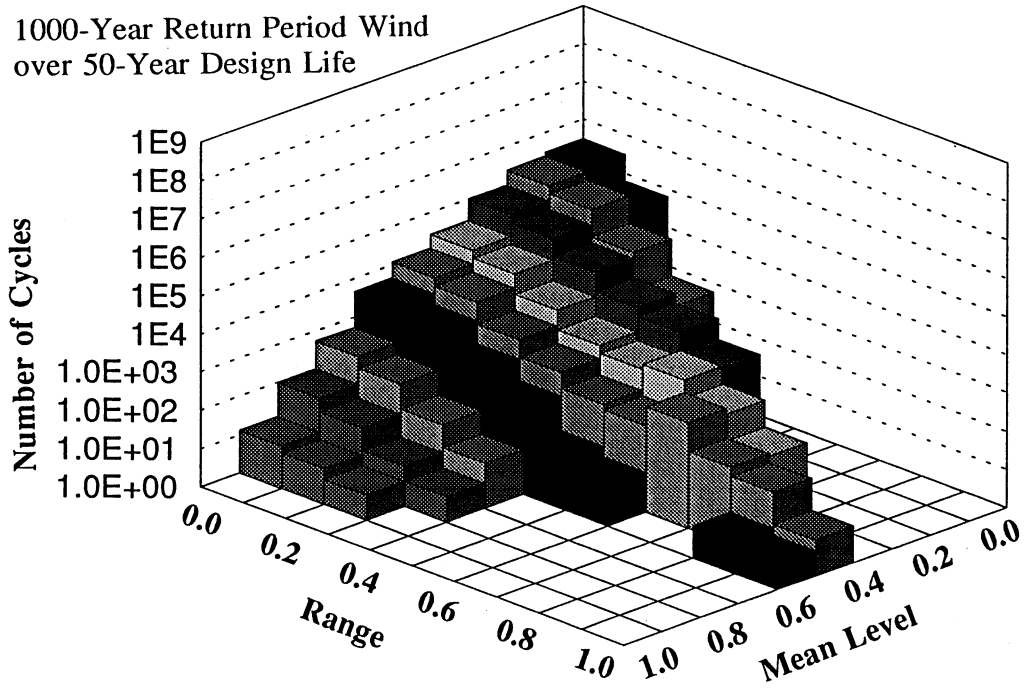

FIG.4.6 TOTAL LOAD CYCLE DISTRIBUTION OF TAP 50501 IN REGION C

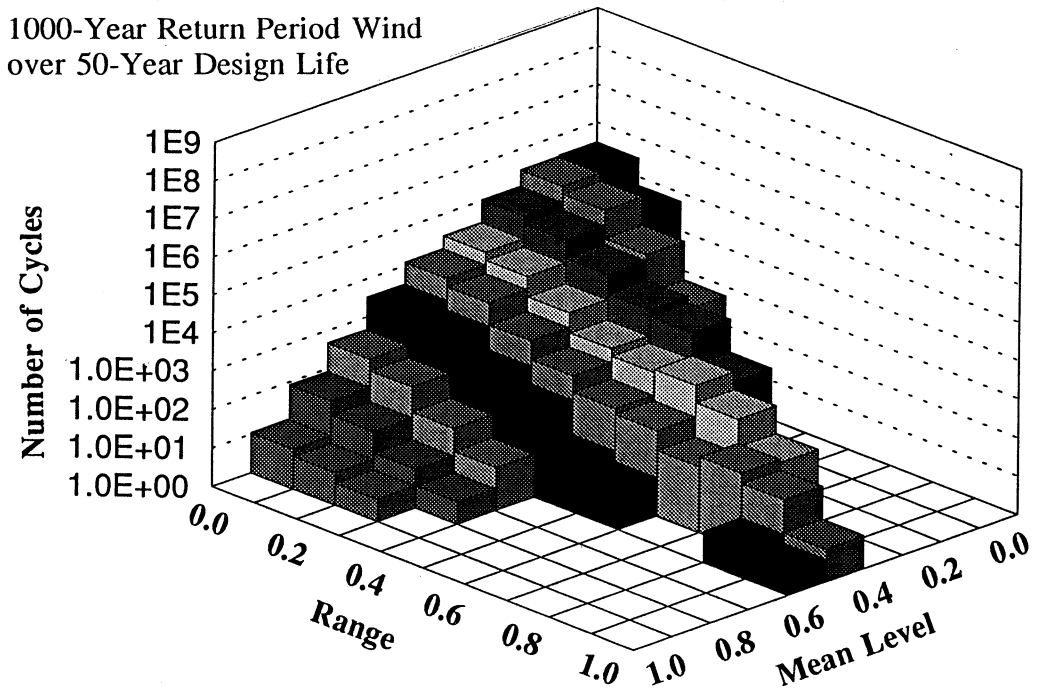

FIG.4.7 TOTAL LOAD CYCLE DISTRIBUTION OF TAP 50501 IN REGION D

4.4 Mean Levels of Load Cycles

Total load cycle distribution is a joint distribution in which total load cycles are distributed over both cycle ranges and mean levels. It is ideal to directly use the total load cycle distributions for the fatigue tests of roof cladding. However, such a test may be very expensive and sometimes it is impossible due to the limitation of test equipment. Therefore some rational simplification of total load cycle distributions is desirable. An immediate idea is to simplify the distribution over cycle mean levels since it is well known that the effect of cycle mean levels on the total fatigue damage of roof cladding is much less than that of cycle ranges.

A kind of diagram is designed to analyse the total load cycle distribution with respect to cycle mean levels only. Such diagrams are shown in Figs. 4.8 to 4.10 for the three taps, respectively, in Region C with a design gust wind speed of 57 m/s and a design life of 50 years. The number in a cell is a proportion of cycle numbers in the cell to the total cycle numbers in the column which the cell belongs to. The plus sign in a cell indicates that the proportion in this cell is less than 10% but larger than 0. The solid oblique line shown in the diagram represents a particular case, in which the cycle mean level is always the half of the given cycle range. This line has been adopted in some of the existing load cycle distributions.

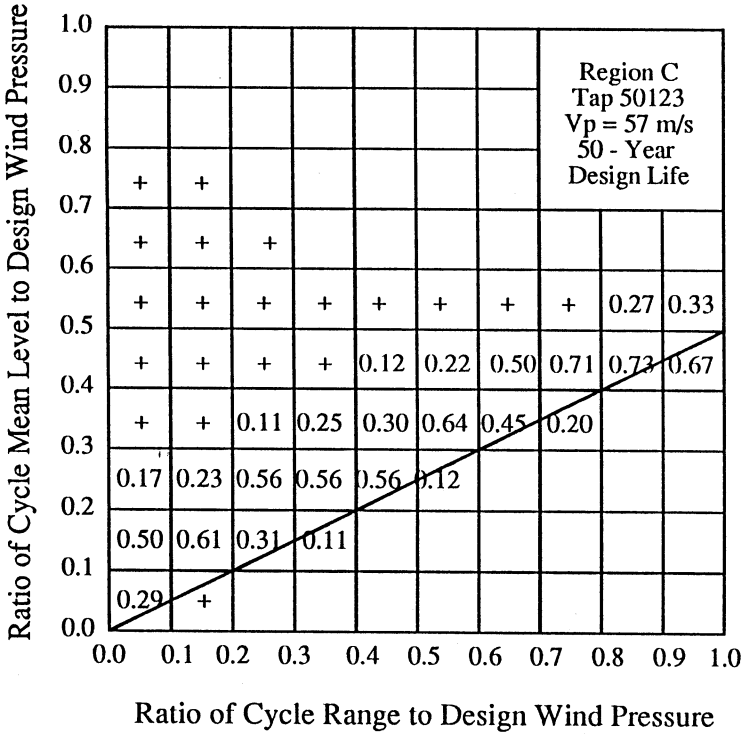

FIG.4.8 CONCENTRATION OF CYCLES WITH RESPECT TO CYCLE MEAN LEVELS---TAP 50123

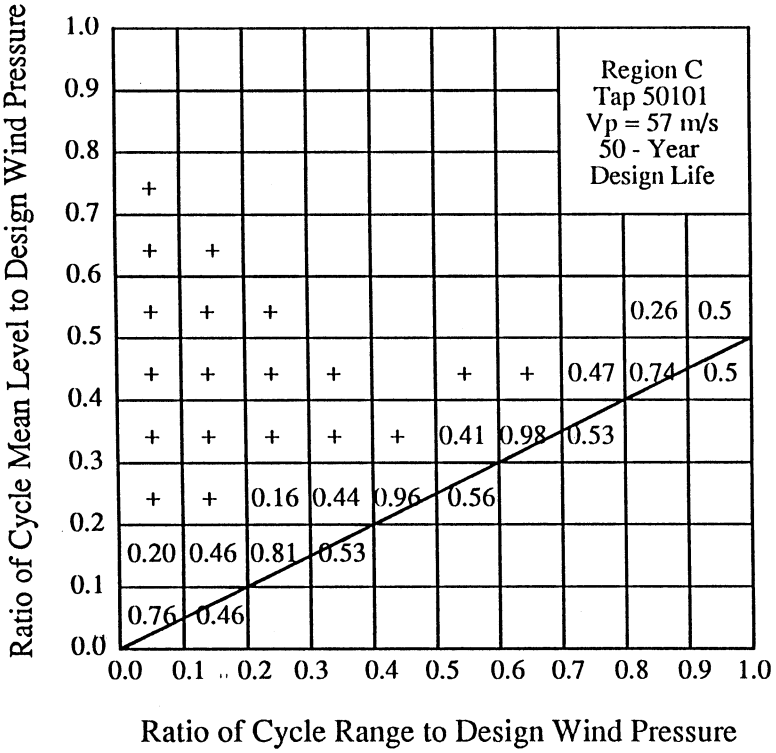

FIG.4.9 CONCENTRATION OF CYCLES WITH RESPECT TO CYCLE MEAN LEVELS---TAP 50101

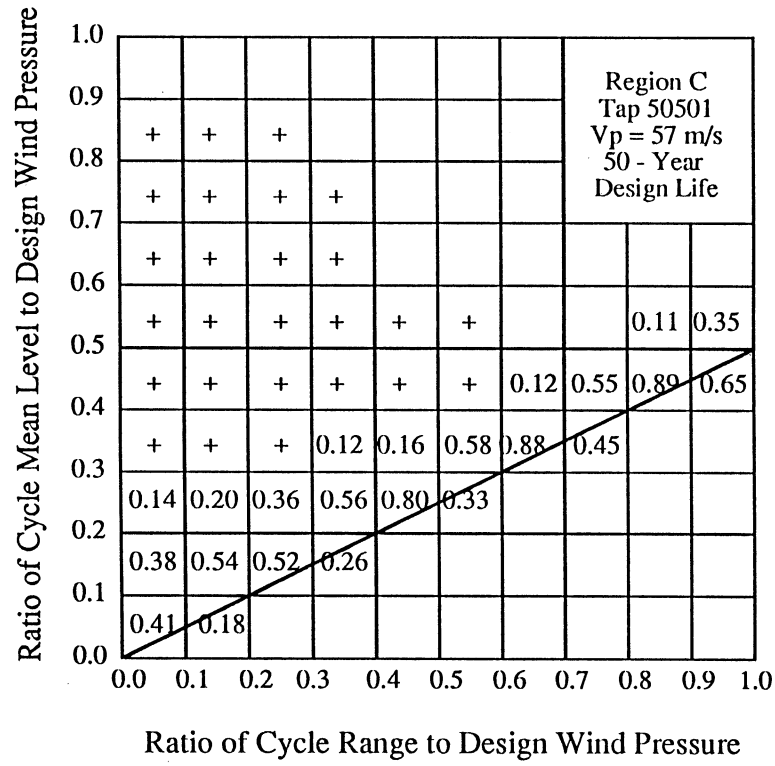

FIG.4.10 CONCENTRATION OF CYCLES WITH RESPECT TO CYCLE MEAN LEVELS---TAP 50501

It is interesting to note that for a given cycle range, especially for cycle ranges of high values, most of the cycles in the corresponding column are distributed in the cells around the solid oblique line. This is particularly obvious in the case of the tap 50101. Therefore, an approximate solution could be reached that for a given cycle range, the mean level of load cycles could be approximately regarded as the half of the cycle range. This approximation coincides with TR440 and DABM load cycle distributions for roof cladding. In this way, only a few block tests are needed instead of a large quantity of block tests with different cycle ranges and cycle mean levels.

Another method for determining an equivalent cycle mean level for a given cycle range comes from statistical average concept. In this statistical average method, the equivalent cycle mean level is a statistical average of the cycle mean levels, Es_i, which can be calculated using the following equation.

$$Es_j = \frac{\sum_{i=1}^{K} s_i N(i,j)}{\sum_{i=1}^{K} N(i,j)} \qquad j=1,2,...L \tag{4.11}$$

in which the N(i,j) is the number of cycles in the cell (i,j) of the total load cycle distribution; s_i is the largest mean level of cycles in the cell (i,j); K is the number of cells with respect to cycle mean levels whilst L is the number of cells with respect to cycle ranges.

The results obtained by using the above equation are shown in Fig. 4.11 together with the solid oblique line for all the three taps in Region C with a design gust wind speed of 57 m/s and a design life of 50 years. It is seen that the equivalent mean levels (i.e, the statistical average mean levels) are in general higher than those provided by the solid line. In the case of the tap 50101, the equivalent cycle mean levels are more close to the solid line than the other two taps. The difference between the equivalent mean levels and the solid line becomes less in the cycle ranges of high values. This difference may not cause any significant problem in high-cycle fatigue. However, for low-cycle fatigue problem, it is better to use the equivalent mean levels obtained from the statistical average method than to simply use the solid oblique line.

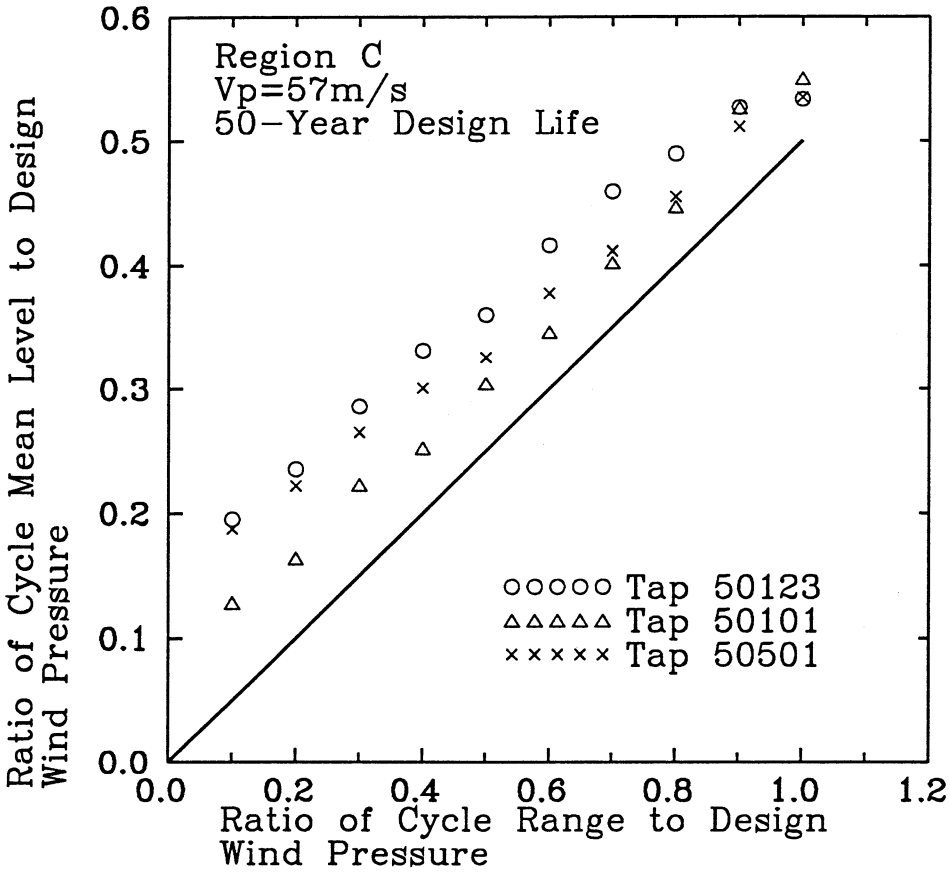

FIG.4.11 EQUIVALENT MEAN LEVELS OF LOAD CYCLES

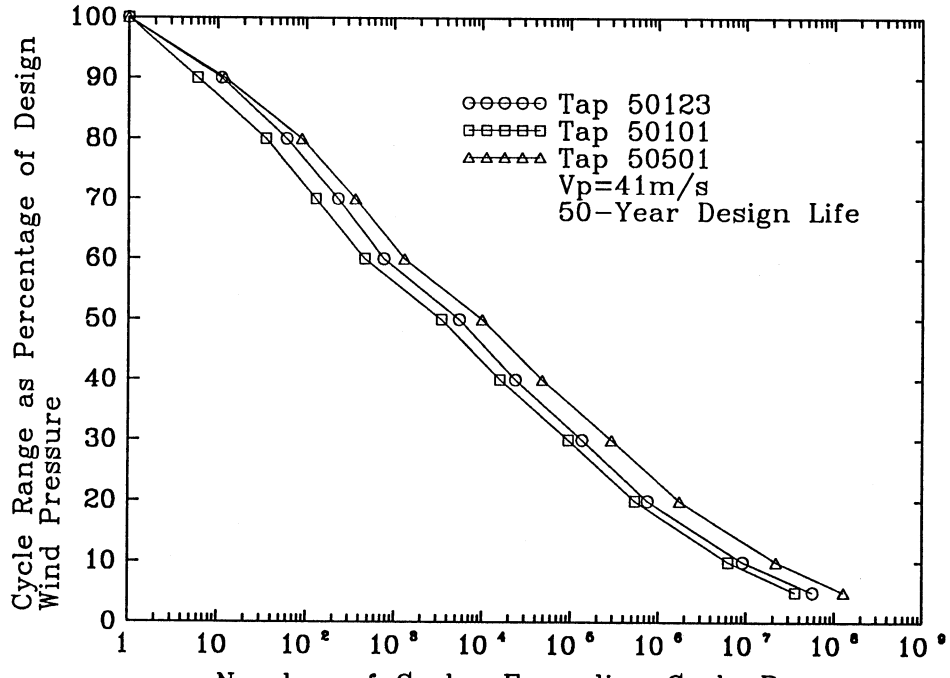

FIG.4.12 DISTRIBUTIONS OF CYCLE RANGES FOR THREE TAPS IN REGION A

4.5 Distributions of Cycle Ranges

The relationships between cycle range, expressed as percentages of the design wind pressure, and the number of cycles exceeding the cycle range are shown in Fig. 4.12 for all the three taps in Region A with a permissible design wind speed of 41 m/s and a design life of 50 years. It can be seen that as the cycle range becomes small, the cycle number increases very rapidly. It is clear that the three taps of concern have different cycle numbers for a given cycle range. The tap 50501 has both the largest cycle number and the largest design wind pressure. Therefore, the tap 50501 represents a most critical case as far as fatigue design is concerned.

For the tap 50501 in different regions with different permissible design wind speeds, the relationships between cycle range and number of cycles exceeding the cycle range are plotted in Fig. 4.13 for a 50-year design life. Since the accumulations of cycles in both Region C and Region D are from a few cyclones whilst that in Region A is from hour to hour, the total number of cycles for Region A are much larger than those for Regions C and D, particularly in the cycle range of low levels. The number of cycles for Region C, however, is nearly the same as that for Region D.

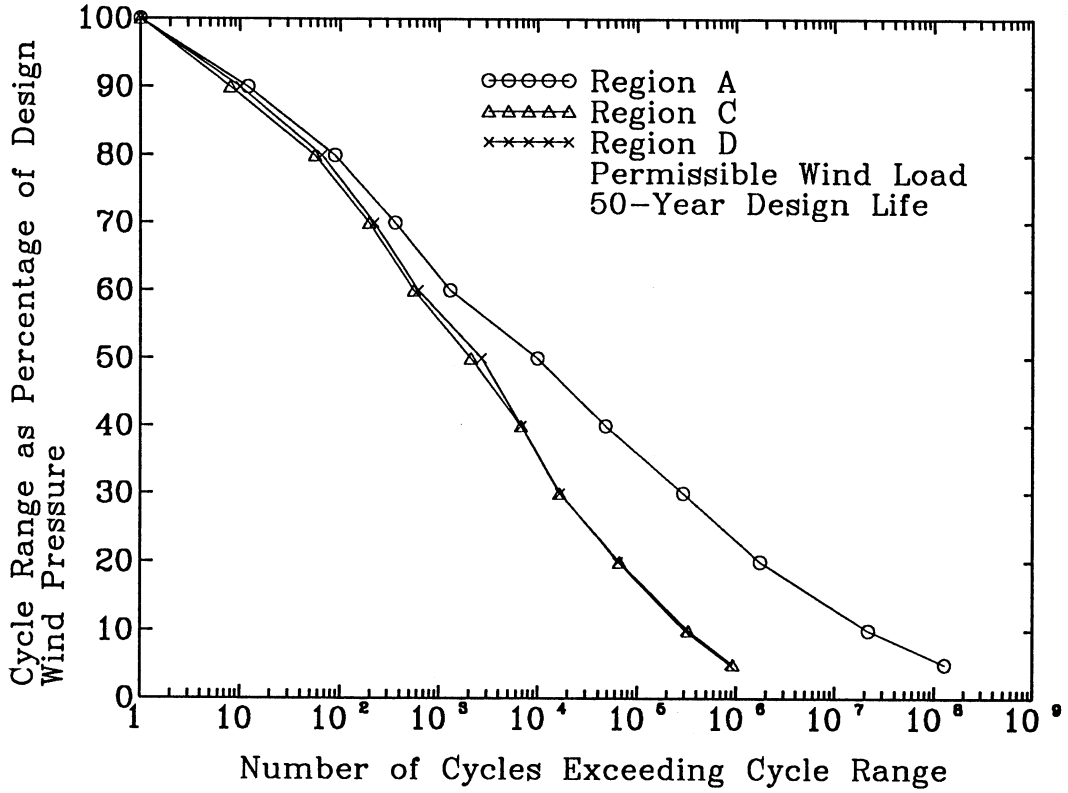

FIG.4.13 DISTRIBUTIONS OF CYCLE RANGES OF TAP 50501 IN THREE REGIONS

Noted that the permissible design wind pressure for Region D is larger than that for Region C. Therefore, for the same percentage of the design wind pressure, the actual cycle range is larger for Region D than for Region C. Furthermore, for the same hysteresis threshold of 0.05 of the design wind pressure, more cycles would be cut in the case of Region D. Nevertheless, when fatigue damage of roof cladding is estimated, the final hysteresis threshold is decided by the endurance limit of the roof cladding itself. This endurance limit is usually much higher than 0.05 of the design wind pressure and it is independent of wind regions.

The distribution of cycle ranges is also computed for different design life of roof cladding associated with different design wind pressures. Figs. 4.14 to 4.16 show the distributions of cycle ranges for the tap 50501 in Region A, C and D, respectively. The design life is 20, 50, and 100 years, respectively, in which the gust wind speed of 20, 50, and 100-year return period is assumed to occur once in the corresponding design life. The general conclusion is that as the wind return period (or design life) increases, the number of cycles increases. Although the cycle number in the cycle range of high values seems not to increase very much, the actual cycle ranges determined by the design wind pressure would be much larger when the wind return period (or design life) becomes larger. Therefore, significant difference of fatigue damage to roof cladding is expected between the 20-year and 100-year design life.

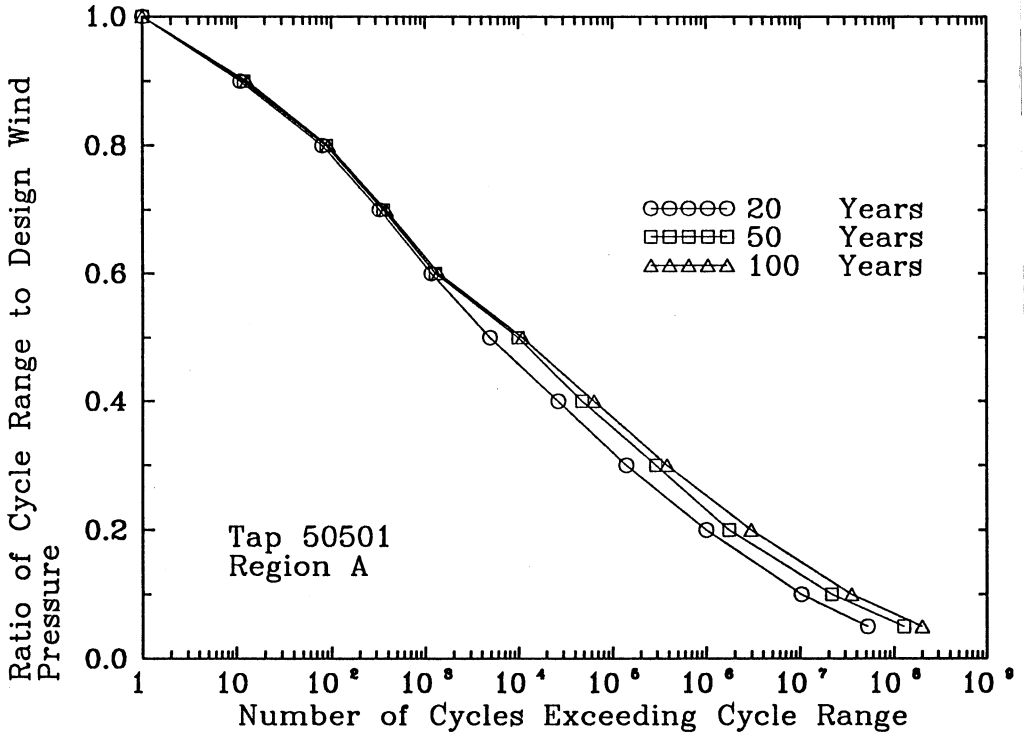

FIG.4.14 EFFECTS OF ROOFING DESIGN LIFE FOR TAP 50501 IN REGION A

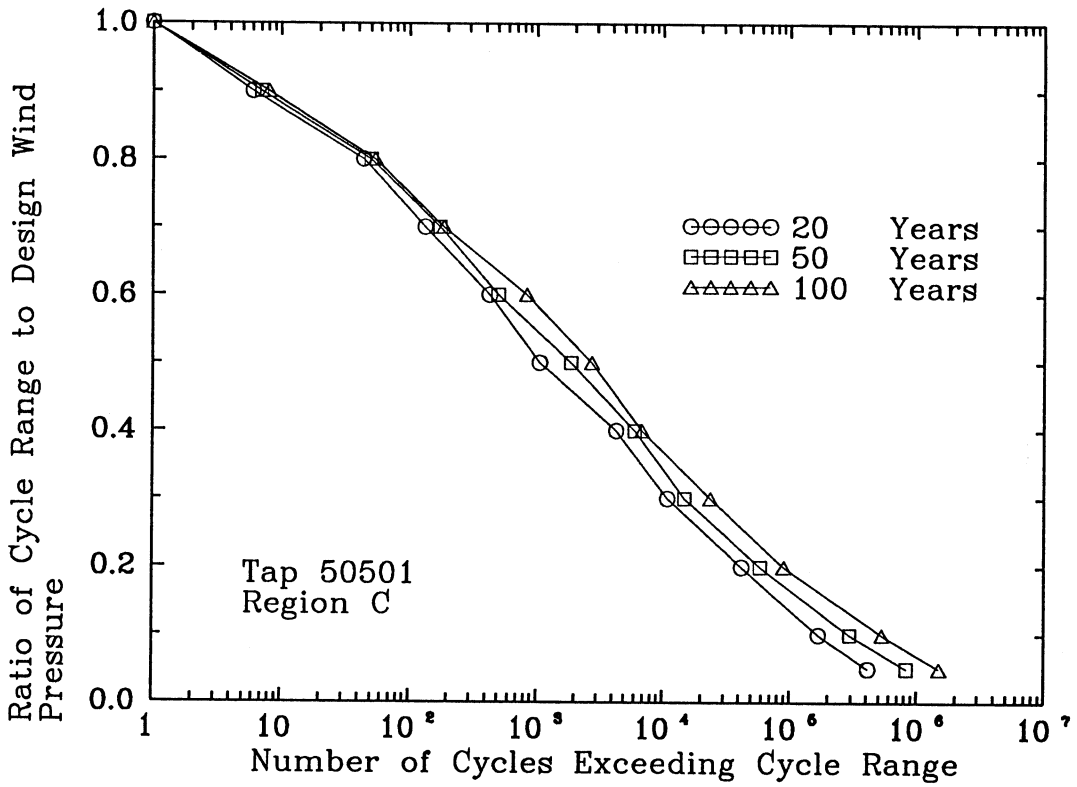

FIG.4.15 EFFECTS OF ROOFING DESIGN LIFE FOR TAP 50501 IN REGION C

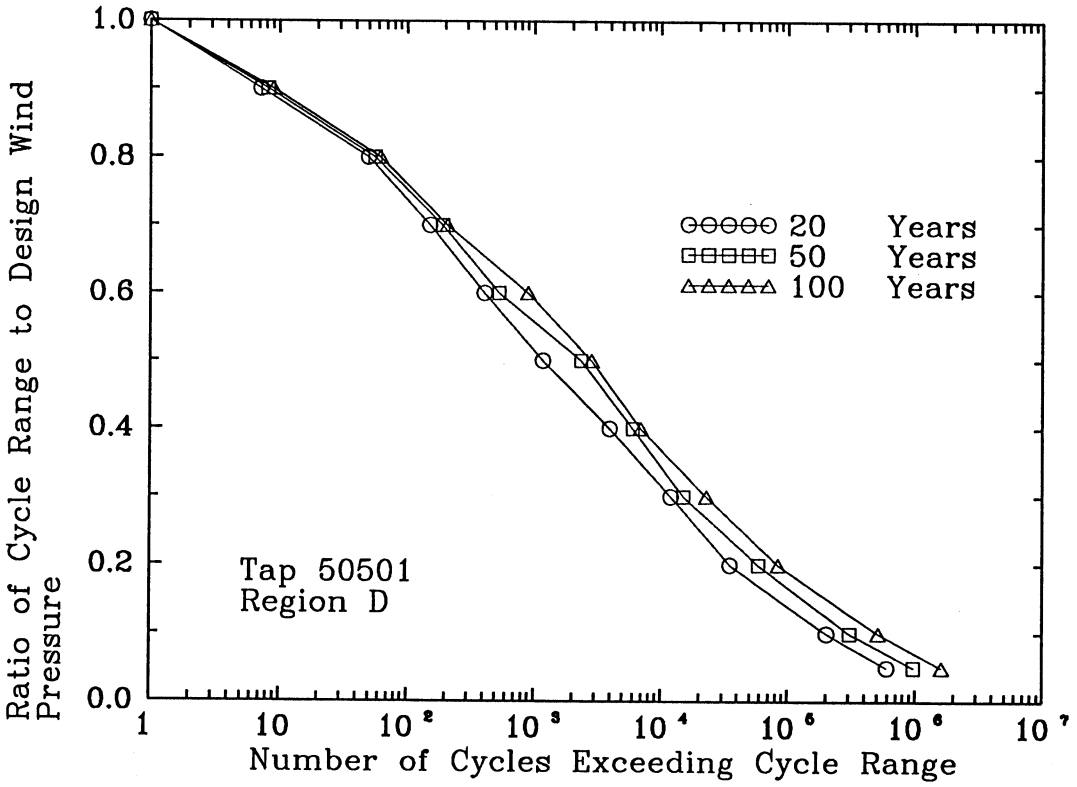

FIG.4.16 EFFECTS OF ROOFING DESIGN LIFE FOR TAP 50501 IN REGION D

As mentioned in Section 4.1 about wind climate in Region A, the sensitivity of load cycle distributions to the parameter k is assessed. Fig. 4.17 shows the load cycle distributions of the tap 50501 in Region A for k=1.5, 2.0 and 2.5. It can be seen that as the parameter k increases, the number of cycles increases. As the cycle range becomes small, the difference in cycles becomes large. Therefore, it is important to determine the parameter k with a careful consideration of actual local wind climate.

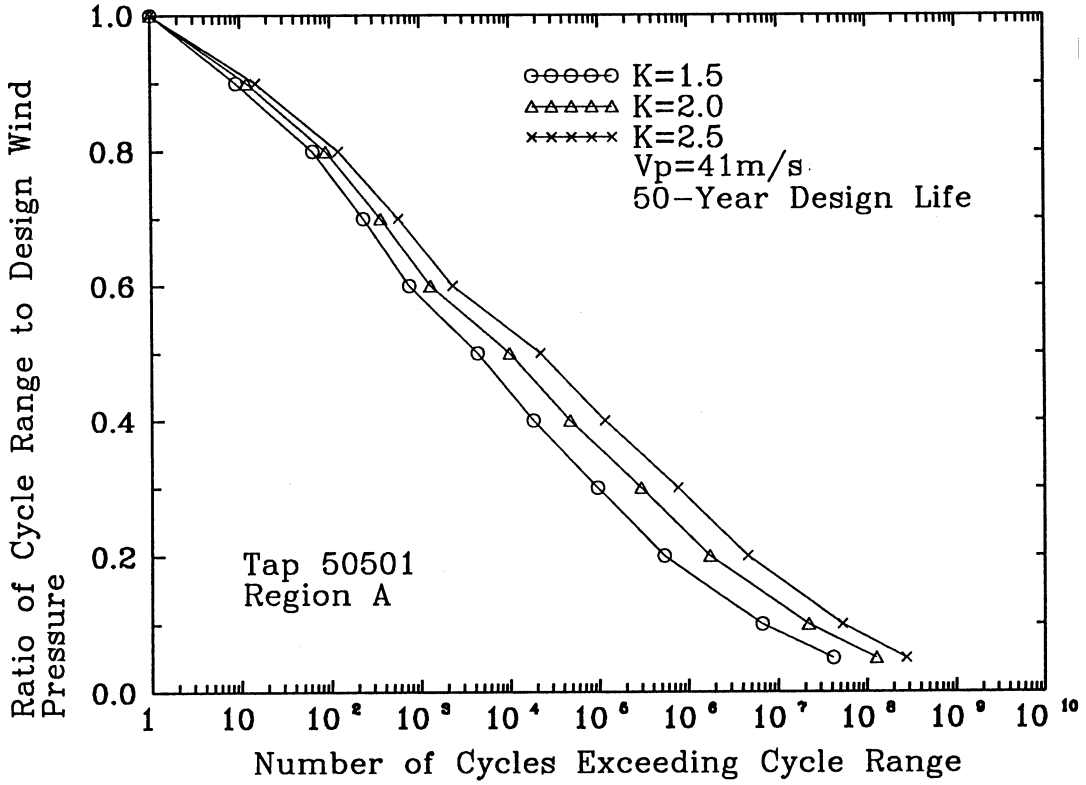

FIG.4.17 EFFECTS OF PARAMETER k ON DISTRIBUTION OF CYCLE RANGE

5 COMPARISON OF LOAD CYCLE DISTRIBUTIONS

5.1 Comparison with European recommendations

Only the distribution of cycle ranges for the tap 50501 is considered to compare with European recommendations since this tap produces the most energetic fatigue loading. The ECCS and BRE distributions of cycle ranges are represented in Fig. 5.1 together with that of the tap 50501 for a temperate region, a 50-year wind return period and a 50-year design life. It is seen that the ECCS and BRE recommendations underestimate the number of cycles in the ranges from 30% to 90% of the design wind pressure. However, in the

cycle range of very low value, the number of cycles computed by the present method are nearly the same as those predicted by the ECCS recommendation. It should be noted that in the present method the effects of wind direction on cycle distributions are not considered.

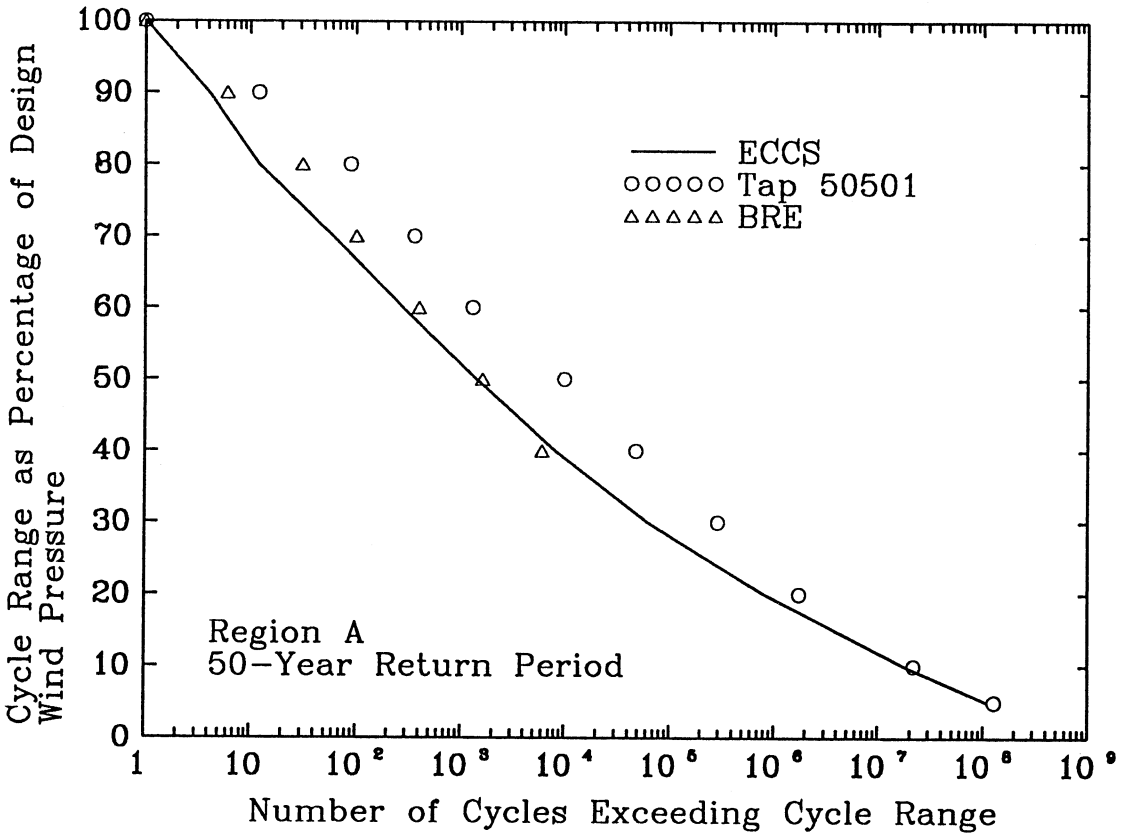

FIG.5.1 COMPARISON OF ECCS AND BRE WITH PRESENT RESULTS

When comparing the cycle range distributions of the tap 50501 in Regions C and D with the ECCS distribution, a significant difference appears, as shown in Fig. 5.2. In the cycle range of high values, the number of cycles computed by the present method is more than those predicted by the ECCS method, and in the cycle range of low values, the situation is reversed. This difference is attributed to wind climates concerned, which lead to different long-term effects. It is clear that for a cyclone prone area, the low cycle fatigue problem appears to be dominant for the light gauge steel profiled roofing sheets.

Fig. 5.3 shows the cycle distribution of the wind pressure given in the draft of the German Wind Loading Code (FRG recommendation, Gerhardt

and Kramer, 1986), as mentioned in Section 1.2. The distribution is reproduced here in terms of the number of cycles exceeding cycle range expressed as percentage of the design wind pressure. The load cycle distribution of the tap 50501 in Region A with a 50-year wind return period and a 50-year design life is also plotted for comparison. It can be seen that in the cycle range of high value, both distributions coincide with each other. However, in the cycle range of medium value, some difference appears. The German distribution seems to underestimate cycle numbers. In the cycle range of low value, both distributions become close to each other again.

In conclusion, for the critical roof pressures on low-rise buildings in temperate regions with a 50-year return period wind over a 50 year design life, the European recommendations on load cycle distributions seem to underestimate load cycles. The European recommendations could not be used in cyclone regions.

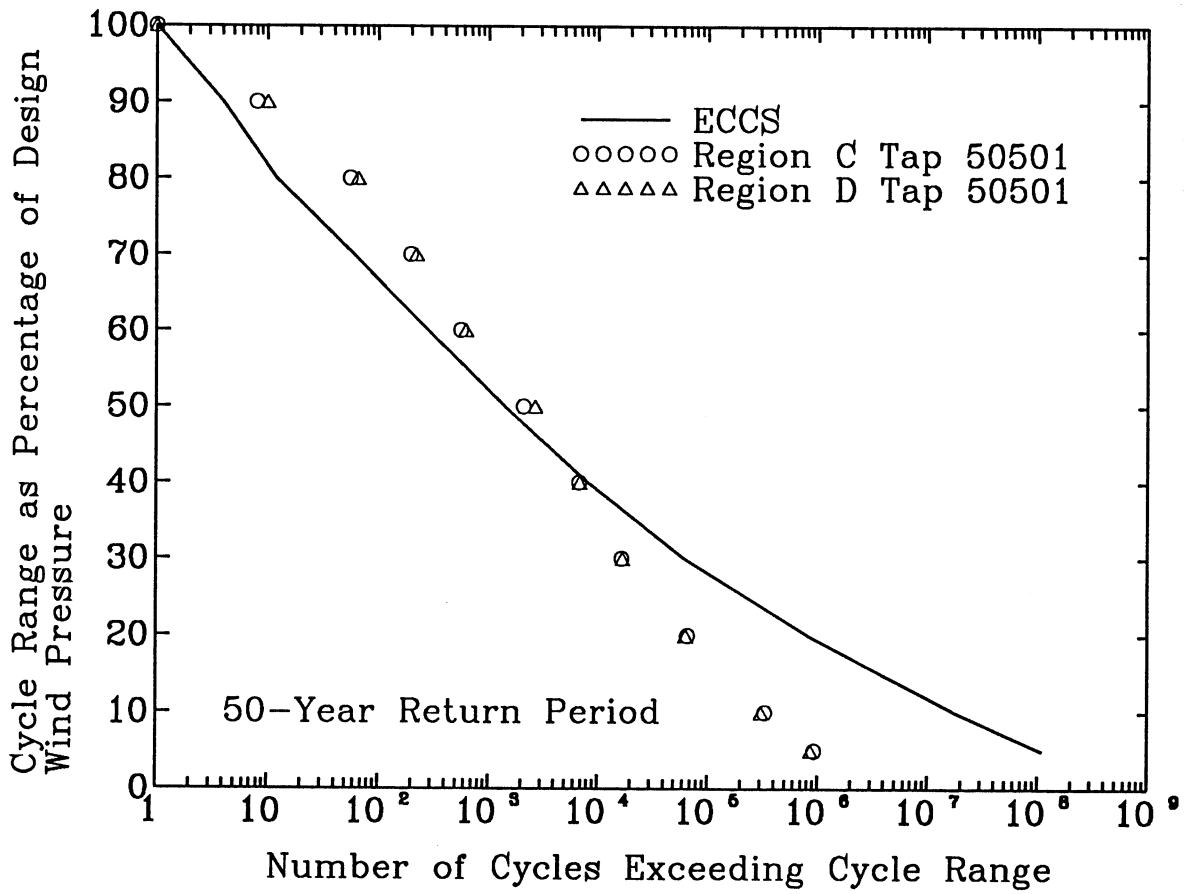

FIG.5.2 COMPARISON OF ECCS WITH PRESENT RESULTS FOR REGION C AND REGION D

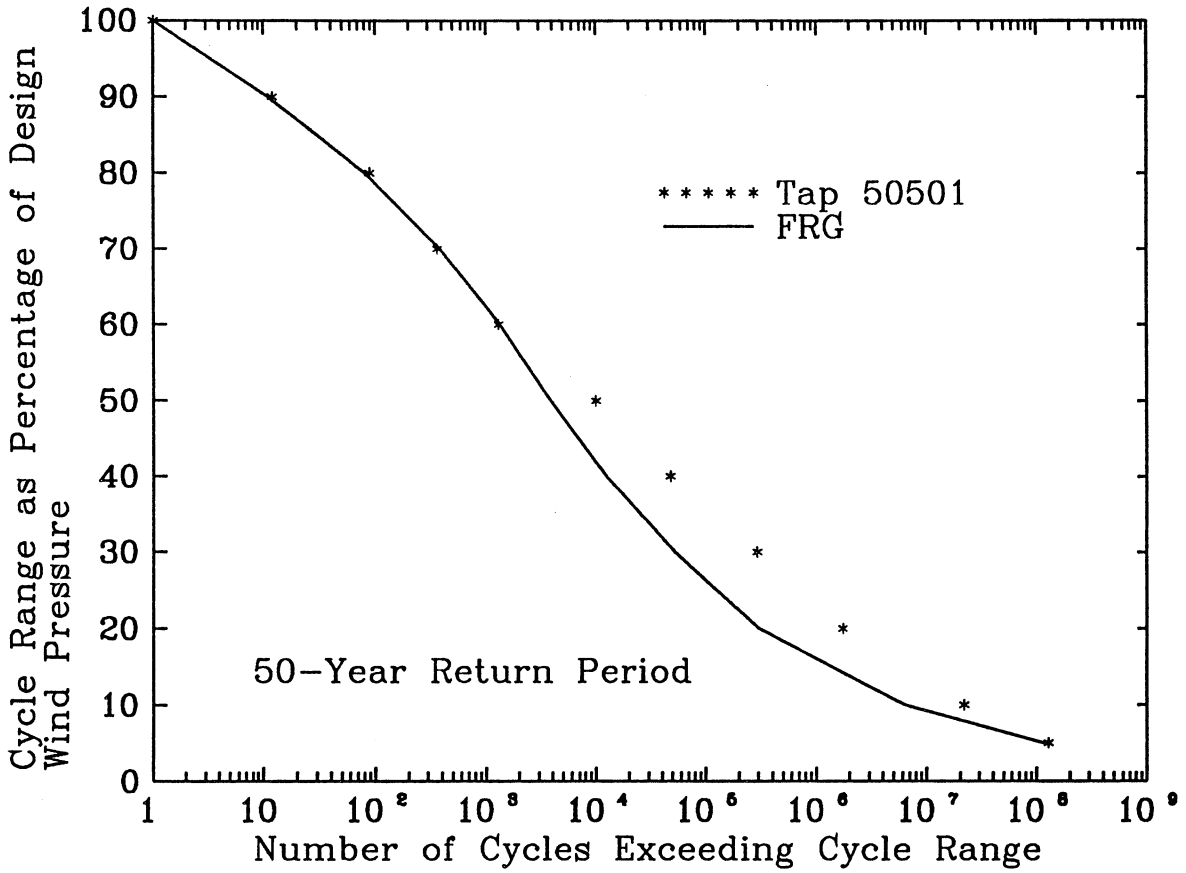

FIG.5.3 COMPARISON OF FRG WITH PRESENT RESULTS FOR REGION A

5.2 Comparison with TR440 and DABM

Both TR440 and DABM load cycle distributions are originally proposed for only one cyclone in Region C or D with a permissible design wind speed and at an open terrain. An overload of 1.8 times the permissible design pressure in DABM and an ultimate load in TR440 follow the cyclic tests with an intention to convert the permissible design to the ultimate design.

Keeping the same design philosophy, one could perform a comparison between TR440 (or DABM) recommendation and the present results. The results in the third row of Table 5.1 is the distribution of cycle ranges for the tap 50501 in Region C Category 2. The number of cycles in each cell of the corresponding total load cycle distribution has been upgraded in Table 5.1 to the nearest 10% of the peak load. The permissible design wind speed is 57

m/s and the duration of each cyclone is three hours. The results in the fourth row of Table 5.1 are obtained based on the same conditions as the third row, except that only one cyclone with a wind speed of 57 m/s and a three-hour duration is considered. The use of the three-hour duration is because the TR440 and the DABM distributions were thought to correspond to the three-hour duration. The TR440 and DABM distributions are listed in the fifth and sixth rows, respectively. The overload is not included in the table.

Assuming that the actual hysteresis threshold is 0.2 of the permissible design wind pressure, one can find that the total cycle number in the fourth row is 10,177, which is nearly the same as the total cycle numbers in the TR440 and the DABM. However, comparing the cycle distribution in the fourth row with the TR440 and the DABM distributions, one can find that the TR440 moderately overestimates the range of cycles, but the DABM extremely overestimates the range of cycles. When comparing the TR440 with the results in the third row which includes the long-term effects, the TR440 slightly overestimates both the cycle number or cycle range in high levels but underestimates the number of cycles in low levels. It is obvious from the comparison of results in the third row and the fourth row that the long-term wind climate significantly affects the number of cycles.

In fatigue tests of roof cladding, the hysteresis threshold should be determined by the fatigue resistance of roof assembly itself. Different roof assemblies may have different hysteresis thresholds or endurance limits. From this point of view, it is better to provide structural engineers with a completed load cycle distribution and let them decide the actual hysteresis threshold based on the characteristics of materials or structures.

In the new version of Australian Wind Loading Code (SAA, 1989), the TR440 in the permissible design form is converted into the ultimate design form, but the actual cycle numbers and cycle ranges are unchanged. The design philosophy behind this is that the ultimate fatigue damage to roof cladding is attributed to one cyclone with a wind speed of 1000-year return period during the 50-year design life of roof cladding. The fourth row of Table 5.2 shows the distribution of cycle ranges for the tap 50501 in Region C Category 2, considering only one cyclone with a wind return period of 1000 years and a three-hour duration. The third row shows the same results for the tap 50501 but considering the long-term effect of wind climate of a 1000-year return period over a 50-year design life.

Comparing the results in the fourth row with the TR440, one can find that

TABLE 5.1 Comparison of Distributions of Cycle Ranges in Region C (Permissible Design Criteria)

Cycle range (1)	0.1 (2)	0.2 (3)	0.3 (4)	0.4 (5)	0.5 (6)	0.6 (7)	0.7 (8)	0.8 (9)	0.9 (10)	1.0 (11)
	The number of cycles									
Tap 50501 (50-year design life)	894,000	396,000	74,500	14,600	6,960	2,300	542	212	71	13
Tap 50501 (One cyclone)	29,795	18,074	5,816	2,399	1,066	494	249	92	48	13
TR440						8,000 (0.625)	2,000 (0.75)			200
DABM										10,000

TABLE 5.2 Comparison of Distributions of Cycle Ranges in Region C (Ultimate Design Criteria)

Cycle Range (1)	0.1 (2)	0.2 (3)	0.3 (4)	0.4 (5)	0.5 (6)	0.6 (7)	0.7 (8)	0.8 (9)	0.9 (10)	1.0 (11)
	The number of cycles									
Tap 50501 (50-year design life)	1,100,000	487,000	91,500	18,000	8,550	2,820	665	260	87	15
Tap 50501 (One cyclone)	36,590	22,209	7,146	2,949	1,311	606	306	114	60	15
TR440				8,000	2,000		200			1
DABM							10,000			1

TABLE 5.3 Comparison of Distributions of Cycle Ranges between Region C and Region D (Ultimate Design Criteria)

Cycle Range (1)	0.1 (2)	0.2 (3)	0.3 (4)	0.4 (5)	0.5 (6)	0.6 (7)	0.7 (8)	0.8 (9)	0.9 (10)	1.0 (11)
	The number of cycles (one cyclone, 2-hour duration)									
Region C	24,393	14,806	4,764	1,966	874	404	204	76	40	10
Region D	29,620	17,979	5,785	2,387	1,061	491	248	92	49	12
	The number of cycles (50-year design life, 2-hour duration)									
Region C	732,000	324,000	61,000	12,000	5,700	1,880	444	173	58	11
Region D	688,000	298,000	57,800	12,300	5,090	2,540	490	192	68	13

the TR440 greatly underestimates the number of cycles above 0.5 of the ultimate design pressure. The DABM seems to be better in such a case from the safety point of view. When comparing the results in the third row with the results in the fourth row, effects of the accumulation of cyclones become extremely obvious. It is clear that if the long-term effect of wind climate is considered, the TR440 distribution becomes certainly unconservative.

Table 5.3 shows the distributions of cycle ranges for the tap 50501 in both Regions C and D in consideration of ultimate design criteria. The duration of one cyclone is 2 hours. When only one cyclone is considered, the number of cycles in Region D is simply 1.214 times that in Region C. When the long-term effects are considered, the number of cycles of high ranges is slightly more in Region D than in Region C, but the situation is reversed for the number of cycles of low ranges. This difference is attributed to the different design gust wind speeds and different extreme value distributions of cyclones.

From the preceding discussion, it can be seen that distributions of cycle ranges depend on design criteria. If only one design cyclone and the permissible wind pressure are considered, the TR440 and the DABM load cycle distributions are conservative, especially in the case of the DABM. If the ultimate wind pressure and only one design cyclone are considered, the TR440 seems to be more unconservative than the DABM. If the long-term effects of wind climate is considered together with the ultimate wind pressure, the TR440 is certainly unconservative. Therefore, it is imperative to establish fatigue design criteria. Once fatigue design criteria are set up, the corresponding load cycle distribution could be determined by the proposed procedure. However, a scientific fatigue design criteria could be closely related to the reliability analysis of wind-induced fatigue loading, which needs a further study.

6 CONCLUSIONS

The main conclusions derived from the current investigation are as follows:

(1) Critical roof pressures on the Texas Tech Field Building are broad-band non-Gaussian processes. Fisher-Tippet Type 1 extreme value distribution does not well fit all the roof pressures concerned. The rainflow method is therefore used to count load cycles instead of the upcrossing method.

(2) The number of cycles on each pressure tap is approximately proportional to the time and the mean speed of incident wind. The number of cycles and the cycle histogram depend on stochastic characteristics of the roof pressures. It is found that around the roof corner area, a small change of tap positions could cause significant differences in both the cycle number and the cycle histogram.

(3) A procedure is proposed to compute total load cycle distributions in consideration of wind return period, design life of roof cladding, wind speed distribution in temperate region, and extreme value distribution and occurrence rate of tropical cyclones in cyclone regions. The long-term effect of wind climate on fatigue loading characteristics is found to be significant.

(4) The total load cycle distribution of critical roof pressures show that for a given cycle range, the mean levels of most cycles approach the half of the cycle range. Therefore, the TR440 test procedure with respect to the cycle mean levels seems to be reasonable. A more sophisticated method for determining an equivalent mean level for a given cycle range is to use the statistical average of cycle mean levels. Such a simplified procedure provides a convenience and accuracy to low cycle fatigue tests of roof cladding.

(5) The relationship between cycle range, expressed as percentage of the design wind pressure, and cycle number exceeding this cycle range shows that as wind return period (or design life) increases, the number of cycles and the cycle ranges increase rapidly. It is also found that the number of cycles and the distributions of cycle ranges in Region A are significantly different from those in Regions C and D.

(6) For roof pressures in temperate regions with a 50-year return period wind over a 50-year design life, the ECCS and BRE recommendations seem to underestimate the cycle number in high cycle ranges, but in low cycle ranges the cycle number is nearly the same as the present results. The situation is reversed when comparing the present results with the FRG recommendation.

(7) If the permissible fatigue design criterion is considered and the hysteresis threshold of cycle ranges is 0.2 of the permissible design load, the total cycle number from the present study is nearly the same as those in the TR440 and DABM, but the cycle distributions are different. Both the TR440 and DABM overestimate the ranges of cycles. If the long-term effect of wind climate is considered, the TR440 overestimates the cycle number or cycle range in high cycle levels but significantly underestimates the cycle number in low cycle

levels.

(8) If the ultimate fatigue design criterion and only one design cyclone are considered, the TR440 seems to be more unconservative than the DABM. If the long-term effect of wind climate is taken into account, the TR440 becomes obviously unconservative.

(9) Reliability analysis of wind-induced fatigue loading is important so that fatigue design criteria could be decided for roof cladding. Once fatigue design criteria are established, the corresponding load cycle distributions could be provided by the proposed procedure.

7 ACKNOWLEDGMENTS

The author is grateful to the financial support from the industries and through JCU Merit Research Grant. He wishes to thank Technical Director of Cyclone Testing Station, Mr. G.F. Reardon for his encouragement and support, and Dr. G.R. Walker, Chief Research Scientist of CSIRO, for many discussions. Thanks are also due to Professor K. Mehta and B.B. Yeatts of Texas Tech. University for making the full-scale data available, and Dr. J.D. Holmes of CSIRO, and Dr. M. Mahendran of the University of Queensland, Technology, for their valuable comments. Mr D. Henderson, Mr K. Abercombie and Ms W.J. Zhang who prepared most figures in this report are really appreciated.

8 REFERENCES

ASCE Fatigue and Fracture Reliability Committee (1982) "Fatigue reliability: variable amplitude loading", Journal of Structural Division, ASCE, Vol. 108, No. ST1, January, pp. 47-69.

Beck, V.R. and Stevens, L.K. (1976) "Constant repeated loading of corrugated sheeting", Proceedings of Metal Structures Conference, The Institution of Engineers, Australia, November, pp. 40-45.

Beck, V.R. and Stevens, L.K. (1979) "Wind loading failures of corrugated roof cladding", Civil Engineering Transactions, The Institution of Engineers, Australia, Vol.CE 21, No. 1, pp. 45-56.

Beck, V.R. (1978) "Loads - the basis of repeated loading and impact criteria", The Workshop on Design for Tropical Cyclones, James Cook University,

Townsville, Australia, Paper L.

Bishop, N.W.M. (1990) "A theoretical solution for the estimation of rainflow ranges from power spectral density data", Fatigue and Fracture Engineering of Materials and Structures, Vol.13, No.4, pp.311-326.

Chaudhury, G.K. and Dover, W.D. (1985) "Fatigue analysis of offshore platforms subject to sea wave loadings", International Journal of Fatigue, Vol. 7, No.1, pp. 13-19.

Cochran. L.S. and Cermark, J.E. (1992) " Full- and model-scale cladding pressures on the Texas Tech University experimental building", Journal of Wind Engineering and Industrial Aerodynamics, 41-44, pp. 1589-1600.

Cook, N.J. (1990) "The designer's guide to wind loading of building structures", Part-2, Static Structures, Butterworths, London.

Davenport, A.G. (1966) "The estimation of load repetitions on structures with application to wind induced fatigue and overload", Paper presented at the RILEM International Symposium on the Effects of Repeated Loading of Materials and Structures, Mexico City, Mexico.

Davenport, A.G. (1967) "The dependence of wind loads on meteorological parameters", Proceedings of International Conference on Wind Effects on Buildings and Structures, Ottawa, September. Vol.1, pp.19-82.

DABM (1976) "Darwin Area Building Manual", Darwin Reconstruction Commission, Australia.

Dionne, M. and Davenport, A.G. (1988) " A simple relationship between the gust response factor and fatigue damage", Journal of Wind Engineering and Industrial Aerodynamics, 30, pp. 45-54.

Dorman, C.M.L. (1982) "Extreme values - an improved method of fitting", Journal of Wind Engineering and Industrial Aerodynamics, 10, pp. 177-190.

Dorman, C.M.L. (1983) "Tropical cyclone winds: uncertainties in Monte Carlo simulation", Journal of Wind Engineering and Industrial Aerodynamics, 12, pp. 281-296.

Dorman, C.M.L. (1984) "Tropical cyclone wind speeds in Australia", Civil

Engineering Transactions, Institution of Engineers, Australia, Vol. CE26, pp. 132-139.

Dowling, N.E. (1972) "Fatigue failure predictions for complicated stress-strain histories", Journal of Materials, Vol. 7, No. 1, March, pp. 71-87.

Dowling, N.E. and Socie, D.F. (1982) "Simple rainflow counting algorithms", International Journal of Fatigue, Vol. 4, pp. 31-40.

Eaton, K.J. and Mayne, J.R. (1975) "The measurement of wind pressures on two-story houses at Aylesbury", Journal of Wind Engineering and Industrial Aerodynamics, 1, pp. 67-109.

ECCS (1987) "Recommendations for calculating the effects of wind on constructions", Technical Committee 12 -Wind, Report No. 52, Second Edition, Brussels, European Convention for Constructional Steelwork.

Gerhardt, H.J. and Kramer, C. (1986) "Wind induced loading cycle and fatigue testing of lightweight roofing fixations", Journal of Wind Engineering and Industrial Aerodynamics, 23, pp. 237-247.

Gomes, L. and Vickery, B.J. (1978) "Tropical cyclone gust speeds along the Northern Australian Coast", Civil Engineering Transactions, Institution of Engineers, Australia, Vol. CE18, pp. 40-49.

Holmes, J.D. (1993) "Thunderstorm winds and structural design in Australia", Proceedings of the Third Workshop on Wind Engineering, Australian Wind Engineering Society, Brisbane, July, C11-16.

Holmes, J.D., Melbourne, W.H. and Walker, G.R. (1990) "A commentary on the Australian Standard for Wind Loads", Australian Wind Engineering Society.

Jancauskas,E.D.J., Mahendran,M, Walker, G.R., Capitanio, C. and Prien, G.D. (1990) "Computer simulation of the fatigue behaviour of roof cladding during the passage of a tropical cyclone", Proceedings of the 12th Australasian Conference on the Mechanics of Structures and Materials, Brisbane, Australia.

Lambert, M.J., Ogle, M.H. and Smith, B.W. (1988) "Investigation of wind-induced fatigue in tall guyed steel masts", Journal of Wind Engineering and

Industrial Aerodynamics, 30, pp. 55-65.

Levitan, M.L., Mehta,K.C., Vann,W.P. and Holmes, J.D. (1991) "Field measurements of pressures on the Texas Tech Building", Journal of Wind Engineering and Industrial Aerodynamics, 38, pp. 227-234.

Levitan, M.L. and Mehta, K.C. (1992a) "Texas Tech field experiments for wind loads part 1: building and pressure measuring systems", Journal of Wind Engineering and Industrial Aerodynamics, 41-44, pp. 1565-1576.

Levitan, M.L. and Mehta, K.C. (1992b) "Texas Tech field experiments for wind loads part 2: meteorological instrumentation and terrain", Journal of Wind Engineering and Industrial Aerodynamics, 41-44, pp. 1577-1588.

Lin, Y.K. (1967) "Probabilistic theory of structural dynamics", McGraw-Hill Book Co.,Inc., New York, N.Y.

Liu, H. (1991) "Wind Engineering- a handbook for structural engineers", Prentice Hall, Englewood Cliffs, New Jersey.

Lynn B.A. and Stathopoulos, T. (1985) "Wind-induced fatigue on low metal buildings", Journal of Structural Engineering, ASCE, Vol. 111, No.4, April, pp. 826-839.

Mahendran, M. (1990) "Fatigue behaviour of corrugated roofing under cyclic wind loading", Civil Engineering Transactions, I.E.Aust, Vol. CE32, No. 4, pp. 212-218.

Matsuishi,M. and Endo, T. (1968) "Fatigue of metals subjected to varying stress", presented at the Japan Society of Mechanical Engineers, Fukuoka, Japan.

Mayne, J.R. (1979) " The estimation of extreme winds", Journal of Wind Engineering and Industrial Aerodynamics, 5, pp. 109-137.

Mehta, K.C., Levitan, M.L., Iverson, R.E. and McDonald, J.R. (1992) "Roof pressures measured in the field on a low building", Journal of Wind Engineering and Industrial Engineering, 41-44, pp. 182-192.

Melbourne, W.H. (1977) " Loading cycles for simulation of wind loading", Proceedings of Workshop on Guidelines for Cyclone Product Testing and

Evaluation, Experimental Building Station, Department of Housing and Construction, Australia.

Morgan, J.W. and Beck, V.R. (1977) "Failure of steel-metal roofing under repeated wind loading", Civil Engineering Transactions, The Institution of Engineers, Australia, Vol.CE19, No. 1, pp.1-5.

Okada, H. and Ha, Y.C. (1992) " Comparison of wind tunnel and full scale pressure measurement tests on the Texas Tech Building", Journal of Wind Engineering and Industrial Aerodynamics, 41-44, pp. 1601-1612.

Peterka, J.A. and Cermark, J.E. (1975) "Wind pressure on buildings - probability densities", Journal of Structural Division, ASCE, Vol. 101, No. ST6, June, pp.1255-1267.

Peterka, J.A. (1983) "Selection of local peak pressure coefficients for wind tunnel studies of buildings", Journal of Wind Engineering and Industrial Aerodynamics, 13, pp. 477-488.

Redfearn, D. (1984) "A test rig for proof-testing building components against wind loads", BRE Information Paper IP19/84, Building Research Establishment, UK.

Robson, J.D. (1963) "An introduction to random vibration", Edinburgh University Press, UK.

SAA (1989) "AS1170.2 - SAA loading Code, Part 2: wind loads", Standard Association of Australia.

Southern, R.L (1978) "The nature of tropical cyclones-with emphasis on occurrence in the Australian region", The Workshop on Design for Tropical Cyclones, James Cook University, Townsville, Australia, Paper B.

Stathopoulos, T. (1982) "PDF of wind pressures on low-rise buildings", Journal of the Structural Division, ASCE, Vol. 106, No.ST5, May, pp.973-990.

Stathopoulos, T. (1984) "Wind loads on low-rise buildings: a review of the state of the art", Engineering Structure, Vol. 6, April, pp. 119-135.

Surry, D. (1991) "Pressure measurements on the Texas Tech Building: wind

tunnel measurements and comparisons with full scale", Journal of Wind Engineering and Industrial Aerodynamics, 38, pp. 235-247.

TR440 (1978) "Guidelines for the testing and evaluation of products for cyclone prone areas", Technical Record 440, Experimental Building Station, Department of Housing and Construction, Australia.

Vickery, B.J. (1992) "Design criteria for reinforced concrete chimneys under vortex excitation", The Second Workshop on Wind Engineering, Australian Wind Engineering Society, Melbourne, February, pp. 65-68.

Walker, G.R. (1975) "Report on Cyclone Tracy - Effect on Buildings - December 1974", Vol. 1, Australian Department of Housing and Construction, Melbourne.

Wirsching, P.H. and Light, M.C. (1980) "Fatigue under wide band random stresses", Journal of the Structural Division, ASCE, Vol. 106, No. ST 7, July, pp. 1593-1607.

Yeatts, B.B. and Mehta, K.C. (1992) "Field experiments for building aerodynamics", Proceedings of the Second International Colloquium on Bluff Body Aerodynamics and Applications, Melbourne, Australia, December, Session 9B.